The Atmospheric Significance of Water Clusters and Ozone–Water Complexes.

ARTICLE *in* THE JOURNAL OF PHYSICAL CHEMISTRY A · SEPTEMBER 2013

Impact Factor: 2.69 · DOI: 10.1021/jp407282c · Source: PubMed

6 AUTHORS, INCLUDING:

Josep M Anglada
Spanish National Research Council
108 PUBLICATIONS **2,097** CITATIONS
SEE PROFILE

Lyudmila Slipchenko
Purdue University
63 PUBLICATIONS **3,283** CITATIONS
SEE PROFILE

THE JOURNAL OF PHYSICAL CHEMISTRY A

Article

pubs.acs.org/JPCA

Atmospheric Significance of Water Clusters and Ozone−Water Complexes

Josep M. Anglada,*[,†] Gerald J. Hoffman,[‡] Lyudmila V. Slipchenko,[§] Marilia M.Costa,[∥] Manuel F. Ruiz-López,[∥] and Joseph S. Francisco*[,§]

[†]Departament de Química Biològica i Modelització Molecular, IQAC−CSIC, c/Jordi Girona 18, E-08034 Barcelona, Spain

[‡]Department of Chemistry, Edinboro University of Pennsylvania, Edinboro, Pennsylvania 16444, United States

[§]Department of Chemistry, Purdue University, West Lafayette, Indiana 47907-2084, United States

[∥]Equipe de Chimie et Biochimie Théoriques, SRSMC, University of Lorraine, CNRS, BP 70239, 54506 Vandoeuvre-les-Nancy, France

Supporting Information

ABSTRACT: Ozone−water complexes $O_3\cdots(H_2O)_n$ (n = 1−4) have been theoretically investigated using QCISD and CCSD(T) methods along with the 6-311G(2df,2p), 6-311+G(2df,2p), aug-cc-pVDZ, aug-cc-pVTZ, and aug-cc-pVQZ basis sets and extrapolation to CBS limit. For comparison, water clusters $(H_2O)_n$ (n = 1−4) have also been studied at the same level of theory. The ozone−water complexes are held together by a combination of weak specific hydrogen-bonding and van der Waals interactions. Surprisingly, the hydrogen-bonded complexes are not necessarily the most stable ones. In particular, in the most stable 1:1 complex structure the main stabilizing factors come from van der Waals interactions. The high accuracy of the calculated binding energies provides a reliable basis to discuss the abundance of these clusters in the atmosphere. We predict concentrations up to 9.24×10^{15}, 3.91×10^{14}, and 2.02×19^{14} molecules·cm^{-3} for water dimer, trimer, and tetramer in very hot and humid conditions and that the concentrations of these clusters would remain significant up to 10 km of altitude in the Earth's atmosphere. The concentration of $O_3\cdots H_2O$ is predicted to be between 1 and 2 orders of magnitude higher than previous estimation from the literature: up to 5.74×10^8 molecules·cm^{-3} in very hot and humid conditions at ground level and up to 1.56×10^7 molecules·cm^{-3} at 10 km of altitude of the Earth's atmosphere. The concentrations of the other ozone−water clusters, $O_3\cdot\cdot(H_2O)_2$, $O_3\cdots(H_2O)_3$, and $O_3\cdots(H_2O)_4$, are predicted to be very small or even negligible in the atmosphere.

INTRODUCTION

Ozone and water vapor are among the most important species in the Earth's atmosphere. Ozone plays a dual role. In the stratosphere it prevents harmful UV radiation from reaching the Earth's surface, thus protecting living organisms, but in the troposphere it acts as a pollutant, having an oxidizing effect. Therefore, its concentration has become one of the measures used to indicate the air quality worldwide. The chemistry of the production of ozone as well as its reactions with such substances as volatile organic compounds have been extensively studied and modeled.[1] Water vapor is the third most abundant molecule at low altitudes in the Earth's atmosphere and, through its ability to form hydrogen bonds, can modify the chemistry of our atmosphere and act either as a catalyst or as a reactant.[2−7] In addition, ozone and water vapor are both greenhouse gases having a direct impact on climate change.

Gas-phase water can form complexes in the atmosphere with closed shell molecules and radicals. These complexes have a direct effect on the reactivity of the species involved in cluster formation[2−5,8−15] and can also produce changes in its photochemical properties.[4,16,17] For instance, it has been suggested that photolysis of the $O_3\cdots H_2O$ complex constitutes an additional source of hydroxyl radicals in the atmosphere. It has been proposed that up to 15% of the available OH produced with a red-shifted spectrum can be formed this way,[3,6,16,18,19] although recent results from the literature indicate that the OH produced this way is less than this.[20] Moreover, water vapor can form complexes with itself, producing water clusters, a phenomenon which has received much attention in the literature[10,11,21−50] These complexes, and in particular the water dimer, are thought to contribute to the Earth's radiation balance.[5,6,51,52] They contribute to homogeneous condensation[53] and also to atmospheric chemistry.[5,11,54,55] It is worth pointing out here that water dimer has been observed under environmentally relevant conditions.[56,57]

Received: July 23, 2013
Revised: September 9, 2013
Published: September 12, 2013

   dx.doi.org/10.1021/jp407282c | J. Phys. Chem. A 2013, 117, 10381−10396

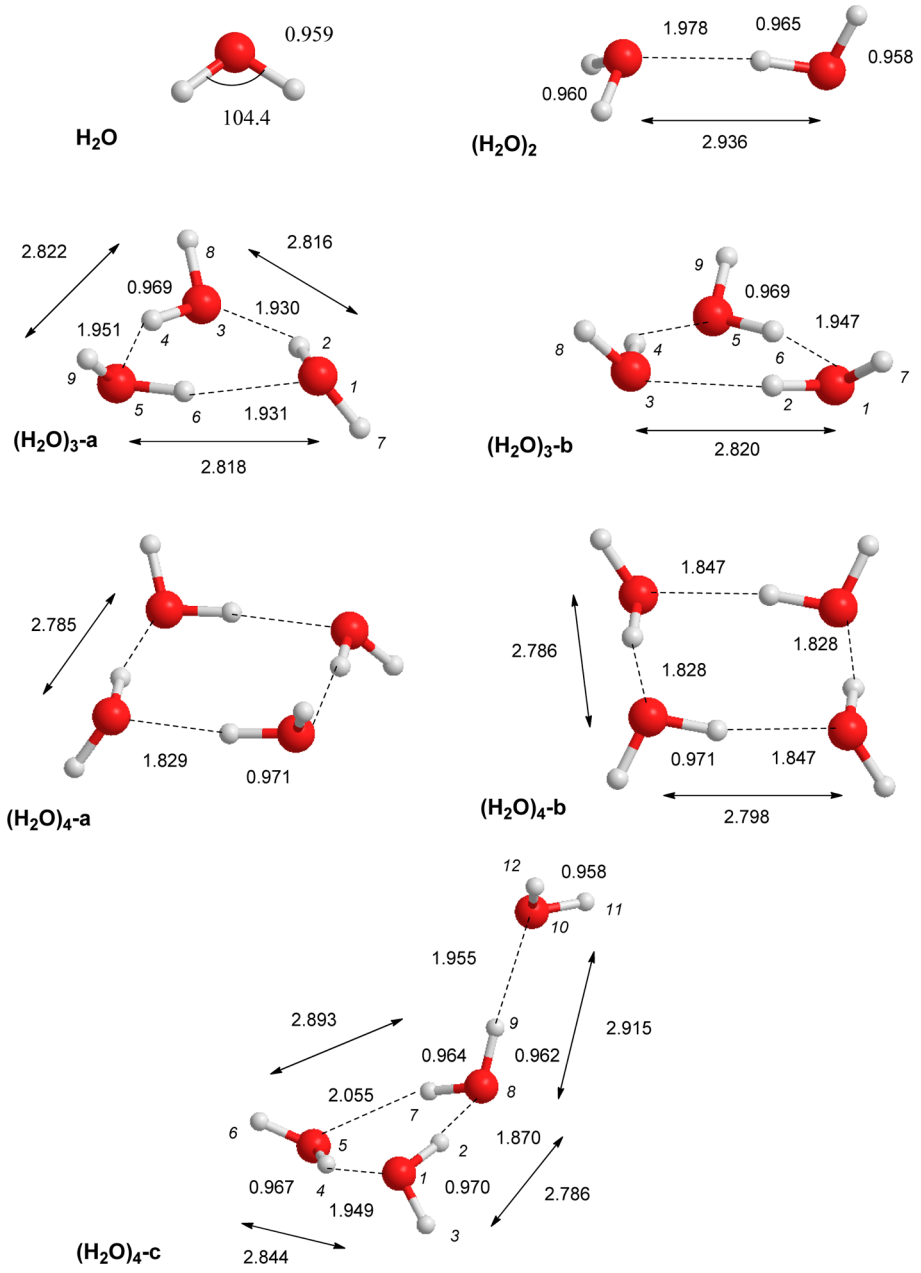

Figure 1. Relevant geometrical parameters for water clusters. Distances are in Angstroms.

The nature of the interaction between water and ozone is of great interest from the perspective of atmospheric chemistry. Many important reactions occur either within or on the surface of aqueous aerosol particles in the atmosphere.[58] While ozone is a polar molecule, its polarity is much less than that of water. Molecular dynamics simulations have revealed low affinity of ozone for water in aqueous solution,[59] in agreement with the positive solvation free energy of O_3 (2.6 kcal·mol^{-1} from Henry law).[60] Moreover, there is a significant free energy minimum for ozone at the surface of water as opposed to within bulk water.[61] This suggests that atmospheric reactions involving ozone may take place on the surface of aqueous aerosol particles rather than inside the bulk. Indeed, it has been shown that ozone reactions taking place at water surfaces are important.[62] In the study of ozone−water complexes, the size of the binding energies and ability of the ozone molecule to incorporate itself among the water clusters can provide clues regarding the solubility of ozone in water.

Given the importance of ozone and water vapor in the Earth's atmosphere and interest in the cluster association of these species, in this work we focused our attention on the investigation of $(H_2O)_n$ (n = 1−4) clusters and formation of complexes between these clusters and an ozone molecule. There have been a number of experimental[19,20,63−66] and computational studies[64,66−73] published on the ozone−water dimer (that is, the complex formed by ozone with one water molecule) but only a few works dealing with ozone and water clusters.[69,72,73] Despite the volume of research, there is a lack of consistency among the various studies regarding the stable structures of the complex, dependent upon the applied computational technique. One of the goals of the work presented here is to definitively identify the stable structures of this dimer as well as the structures of larger such complexes, containing more water molecules. We

dx.doi.org/10.1021/jp407282c | J. Phys. Chem. A 2013, 117, 10381−10396

also aim to investigate the nature of the interactions that hold these clusters together, to report accurate results regarding the binding energies for their formation, and to estimate the concentration of these species in different conditions of the Earth's atmosphere.

COMPUTATIONAL METHODS

In this work a variety of different theoretical approaches were employed for the study of water and ozone−water clusters. In order to determine structures for the ozone−water clusters, we performed, in a first step, Monte Carlo calculations with hybrid quantum mechanics−effective fragment potential (QM/EFP1) approach using the GAMESS software package.[74,75] Water molecules were represented by effective fragments within the original effective fragment potential method (EFP1) framework.[76−78] The EFP1 method is specifically designed for describing interactions in aqueous solutions. Ozone was calculated using density functional theory, with the B3LYP exchange-correlation function[79] and the Dunning−Hay double-ζ basis set with p and d polarization functions.[80] Structures resulting from the Monte Carlo searches were further optimized with equivalent treatment of all atoms in the cluster at the level of second-order Møller−Plesset theory (MP2) using the 6-311+G(d) Pople basis set.[81]

In a second step, all structures were optimized and characterized employing the QCISD approach. In these calculations we used the 6-311G(2df,2p), 6-311+G(2df,2p), aug-cc-pVDZ, and aug-cc-pVTZ basis sets.[82−85] The water dimer, trimer, and $O_3\cdot\cdot(H_2O)_n$ (n = 1−3) have been first optimized and characterized employing aug-cc-pVDZ and then reoptimized using the aug-cc-pVTZ basis set. In the case of $O_3\cdots H_2O$, frequency calculations have been also carried out at the QCISD/aug-cc-pVTZ level of theory. For water tetramer all optimizations and characterizations have been done using the 6-311+G(2df,2p) basis set. The $O_3\cdots(H_2O)_4$ complexes are less relevant for atmospheric purposes and have been optimized and characterized at the QCISD/6-311G(2df,2p) level of theory.

In a third step, in order to obtain accurate binding energies, we performed, at the QCISD-optimized geometries using the largest basis set, single-point energy calculation employing the CCSD(T) method.[86−89] In these calculations we used the aug-cc-pVTZ and aug-cc-pVQZ basis sets,[84,85] and we also considered the extrapolation to the complete basis set limit (CBS) according to the extrapolation scheme by Helgaker et al.[90] CBS results are reported for all water clusters and all $O_3\cdots(H_2O)_n$, n = 1−3 clusters, whereas for the $O_3\cdots(H_2O)_4$ clusters CCSD(T) calculations were done using the aug-cc-pVTZ basis set. In order to check the reliability of the single-determinant-based methods employed in this work, we looked at the T1 diagnostic[91] of the CCSD wave function with regard to the multireference character of the wave function.

All QCISD and CCSD(T) calculations have been carried out using the Gaussian 03 program package.[92] Bonding features have been analyzed according to natural bond orbital analysis (NBO) by Weinhold and co-workers[93] and the atoms in molecules (AIM) theory of Bader.[94] These calculations have been done using the QCISD wave functions obtained with the basis sets indicated in the Supporting Information. In the latter case, the AIMPAC program package has been used.[95] Figures have been done with the Chemdraw[96] and Matplotlib[97] programs.

Additional characterization of intermolecular interactions in the $O_3\cdots(H_2O)_2$ clusters was obtained by means of the general effective fragment potential method (EFP).[76,78,98,99] EFP is a first-principle-based potential that provides a computationally inexpensive way to model intermolecular interactions in noncovalently bound systems. The general EFP method (originally called EFP2) is composed of four interaction terms: Coulomb (electrostatic), induction (polarization), exchange repulsion, and dispersion. All fragments have frozen geometries during the EFP simulations but may orient freely with respect to each other. To account for short-range charge-penetration effects and avoid polarization collapse, Coulomb, polarization, and dispersion interactions were augmented by screening terms.[100−102] Overlap-based electrostatic and dispersion screenings and Gaussian-type polarization screening functions were employed. In this work, effective potentials for water and ozone were constructed using the mixed-basis approach, as previously described.[103] The water potential was the same as that used previously;[104] multipoles for the Coulomb term were obtained in 6-31+G* basis,[105−107] while 6-311++G(3df,2p) basis[108,109] was used for the other terms in water and ozone potentials.

RESULTS AND DISCUSSION

$(H_2O)_n$ (n = 2−4) Clusters. The water dimer, trimer, and tetramer have been extensively studied in the literature (see, for instance, refs 10, 11, 21−46), but in order to analyze ozone−water clusters interactions below and for comparison purposes we summarize the results obtained for $(H_2O)_n$ clusters at the computational level used in our work and comment on some main features. The main geometrical parameters of the optimized geometries are displayed in Figure 1, and Table 1 contains our computed binding energies for successive formation of these clusters.

Water dimer has C_s symmetry, and our calculations predict that the two water molecules are held together by a hydrogen bond having a length of 1.978 Å, while the distance between the two oxygen atoms is computed to be 2.936 Å, in very good

Table 1. Entropies (S in cal·K^{-1}·mol^{-1}) and Relative Energies, Energies Plus ZPE (in kcal·mol^{-1}), Enthalpies, and Free Energies (in kcal·mol^{-1}, at 298 K) Calculated for Formation of the Water Complexes $(H_2O)_n$ (n = 2−4)[a]

compound	S	ΔE	$\Delta(E+\mathrm{ZPE})$	ΔH^0	ΔG^0
$H_2O + H_2O \rightarrow (H_2O)_2$					
$H_2O + H_2O$	90.2	0.00	0.00	0.09	0.00
$(H_2O)_2$	70.3	−5.01	−2.91	−3.33	2.60
$(H_2O)_2 + H_2O \rightarrow (H_2O)_3$					
$(H_2O)_2 + H_2O$	115.4	0.00	0.00	0.00	0.00
$(H_2O)_3$-a	81.5	−10.92	−7.59	−8.78	1.34
$(H_2O)_3$-b	84.2	−10.13	−7.17	−8.12	1.19
$(H_2O)_3 + H_2O \rightarrow (H_2O)_4$					
$(H_2O)_3 + H_2O$	123.7	0.00	0.00	0.00	0.00
$(H_2O)_2 + (H_2O)_2$	140.7	5.79	4.14	5.17	0.09
$(H_2O)_4$-a	92.7	−11.71	−8.84	−9.65	−0.43
$(H_2O)_4$-b	94.5	−10.79	−8.12	−8.85	0.17
$(H_2O)_4$-c	102.7	−5.19	−3.28	−3.38	2.85

[a]The ZPE, S, and enthalpic and entropic corrections correspond to calculations at the QCISD/aug-cc-pVDZ level of theory for $(H_2O)_2$ and $(H_2O)_3$ clusters and at the QCISD/6-311G(2df,2p) level of theory for the $(H_2O)_4$ clusters. Energies correspond to calculations carried out at CCSD(T)/CBS//QCISD/aug-cc-pVTZ for $(H_2O)_2$ and $(H_2O)_3$ clusters and at CCSD(T)/CBS//QCISD/6-311+G(2df,2p) for $(H_2O)_4$ clusters. CBS extrapolation has been done over single-point energy calculations at CCSD(T)/aug-cc-pVTZ and CCSD(T)/aug-cc-pVQZ levels of theory.

dx.doi.org/10.1021/jp407282c | J. Phys. Chem. A 2013, 117, 10381−10396

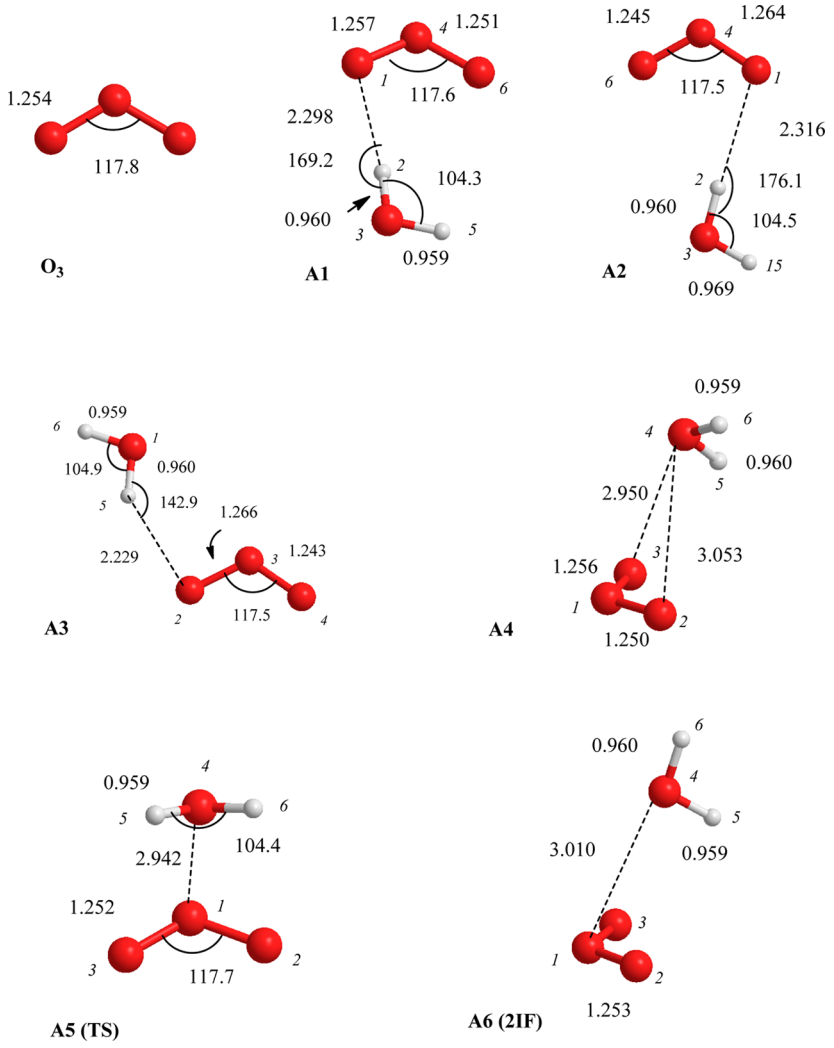

Figure 2. Relevant geometrical parameters for the stationary points in O_3 and $O_3\cdots H_2O$ clusters. Distances are in Angstroms and angles in degrees.

agreement with the 2.976 Å measured experimentally.[110] These geometrical parameters also compare very well with other results from the literature.[10,11,34,36,39,41,111] At our best level of theory, the binding energy and enthalpy at 298 K are computed to be 2.91 and 3.33 kcal·mol^{-1}, respectively, in very good agreement with the experimental values from the literature: $D_o = 3.16 \pm 0.02$ kcal·mol^{-1},[112] $\Delta H° = 3.69 \pm 0.02$ kcal·mol^{-1} at $T = 298$ K;[112] $D_o = 3.15 \pm 0.03$ kcal·mol^{-1},[28] $\Delta H° = 3.59 \pm 0.50$ kcal·mol^{-1} at $T = 358-386$ K;[29] $\Delta H°$ of 3.98 ± 0.90 and 3.58 ± 0.72 kcal·mol^{-1} at $T = 573-723$ and 373−673 K, respectively;[30,31] or $\Delta H°$ of 3.24 ± 0.95 kcal·mol^{-1} at $T = 300$ K.[32] The predicted binding energy also agrees with the results of previous theoretical calculations (in kcal·mol^{-1}: 3.30;[33] 3.01−3.12;[34] 2.99−3.15;[35] and 2.9[10,11,111]). Further insights on the water dimer interaction can be obtained from NBO and topological analysis of the wave function. First, it is interesting to remind the reader that in a given X−H···Y hydrogen bond, where X−H acts as a proton donor and Y as a proton acceptor, there is an electron charge transfer whose direction is reverse to the direction of the proton donation.[113] In the case of the water dimer, NBO analysis leads to a charge transfer of 8.8 me (me stands for millielectron). In addition, topological analysis of the wave function shows that the values of the density and the Laplacian of the density at the bond critical point (bcp) ($\rho = 0.0227$ au and $\nabla^2\rho = 0.0778$ au, see Table S1, Supporting Information; au stands for atomic units) are also in line with the features required for H bonds.[114]

For the water trimer, we considered the two cyclic structures, $(H_2O)_3$-a and $(H_2O)_3$-b, which are held together by three hydrogen bonds, so that each water molecule acts as a H-bond donor and acceptor simultaneously (Figure 1). The two conformers are differentiated from each other by the orientation of the dangling hydrogen atoms. In $(H_2O)_3$-a two dangling hydrogen atoms point to one side and the third one points to the opposite side (we will use the notation *uud* for the dangling hydrogen atoms, where *u* stands for up and *d* stands for down), whereas in $(H_2O)_3$-b the three dangling hydrogen atoms point to the same side (*uuu*). The most stable complex is $(H_2O)_3$-a, for which we computed a binding energy of 7.59 kcal·mol^{-1} and binding enthalpy of 8.78 kcal·mol^{-1} at 298 K with respect to the water dimer plus water monomer reactants. $(H_2O)_3$-b is only slightly less stable ($\Delta(E+ZPE) = 7.17$ kcal·mol^{-1} and $\Delta H°(298\ K) = 8.12$ kcal·mol^{-1}). Despite the fact that the cyclic structure of the trimers forces the nonlinearity of the three hydrogen bonds, the strength of the latter is considerably greater than that of the hydrogen bond in the water dimer. This is reflected in their corresponding bond lengths (about 0.05 Å shorter than in the dimer). Calculated O−O distances (2.819 Å on average) are in very good agreement with the value of 2.85 Å reported by

dx.doi.org/10.1021/jp407282c | J. Phys. Chem. A 2013, 117, 10381−10396

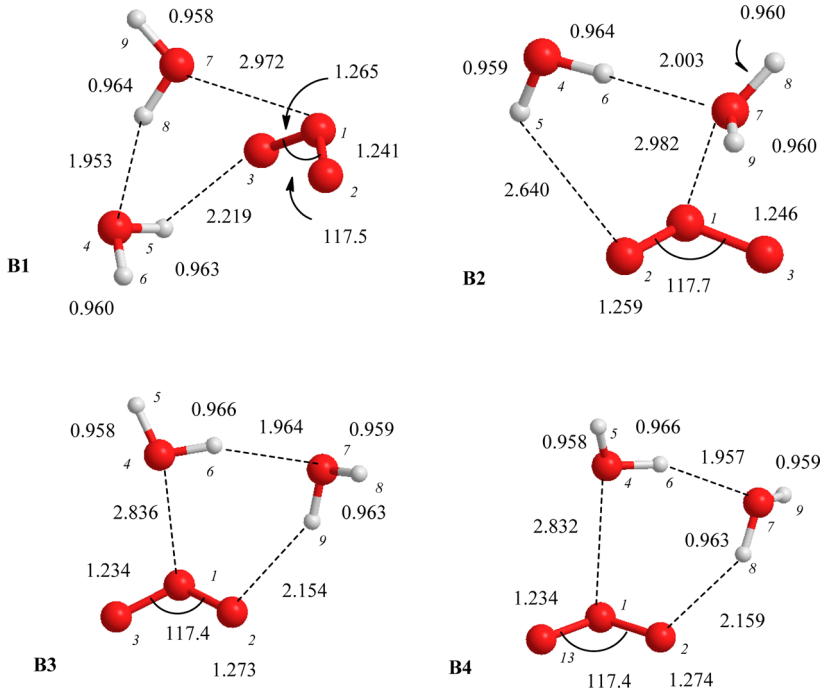

Figure 3. Relevant geometrical parameters for $O_3\cdots 2H_2O$ clusters. Distances are in Angstroms.

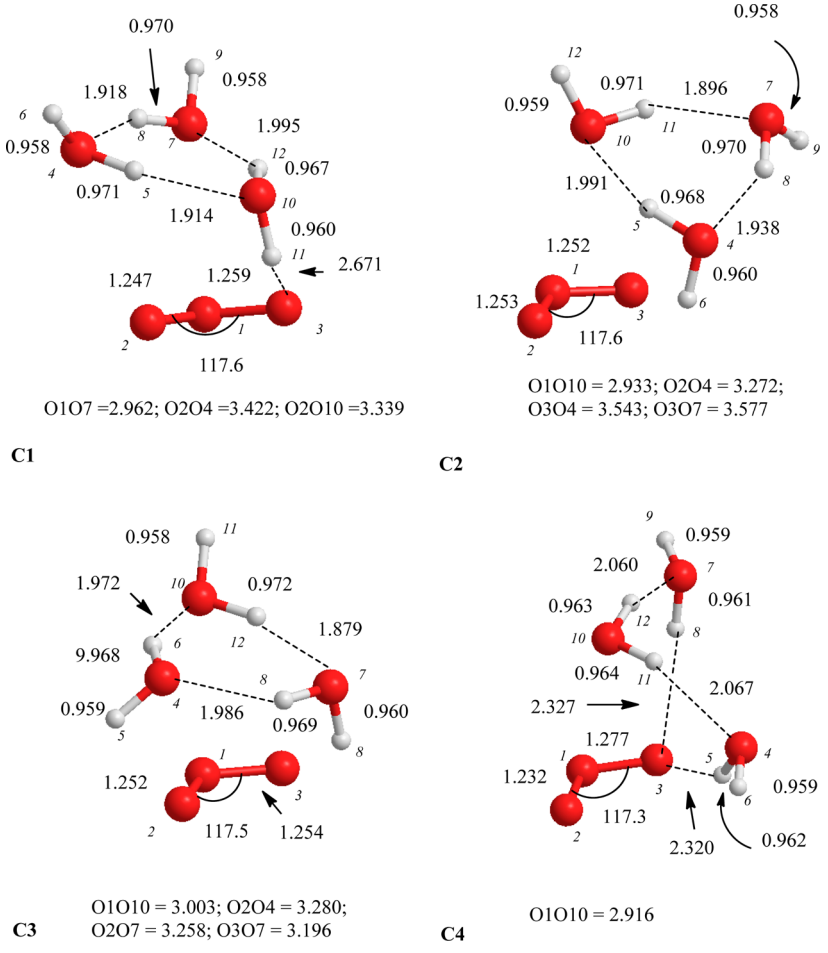

Figure 4. Relevant geometrical parameters for $O_3\cdots 3H_2O$ clusters. Distances are in Angstroms and angles in degrees. For the sake of clarity, the bond lengths of several O··O interactions have not been explicitly drawn but written nearby each structure.

dx.doi.org/10.1021/jp407282c | J. Phys. Chem. A 2013, 117, 10381−10396

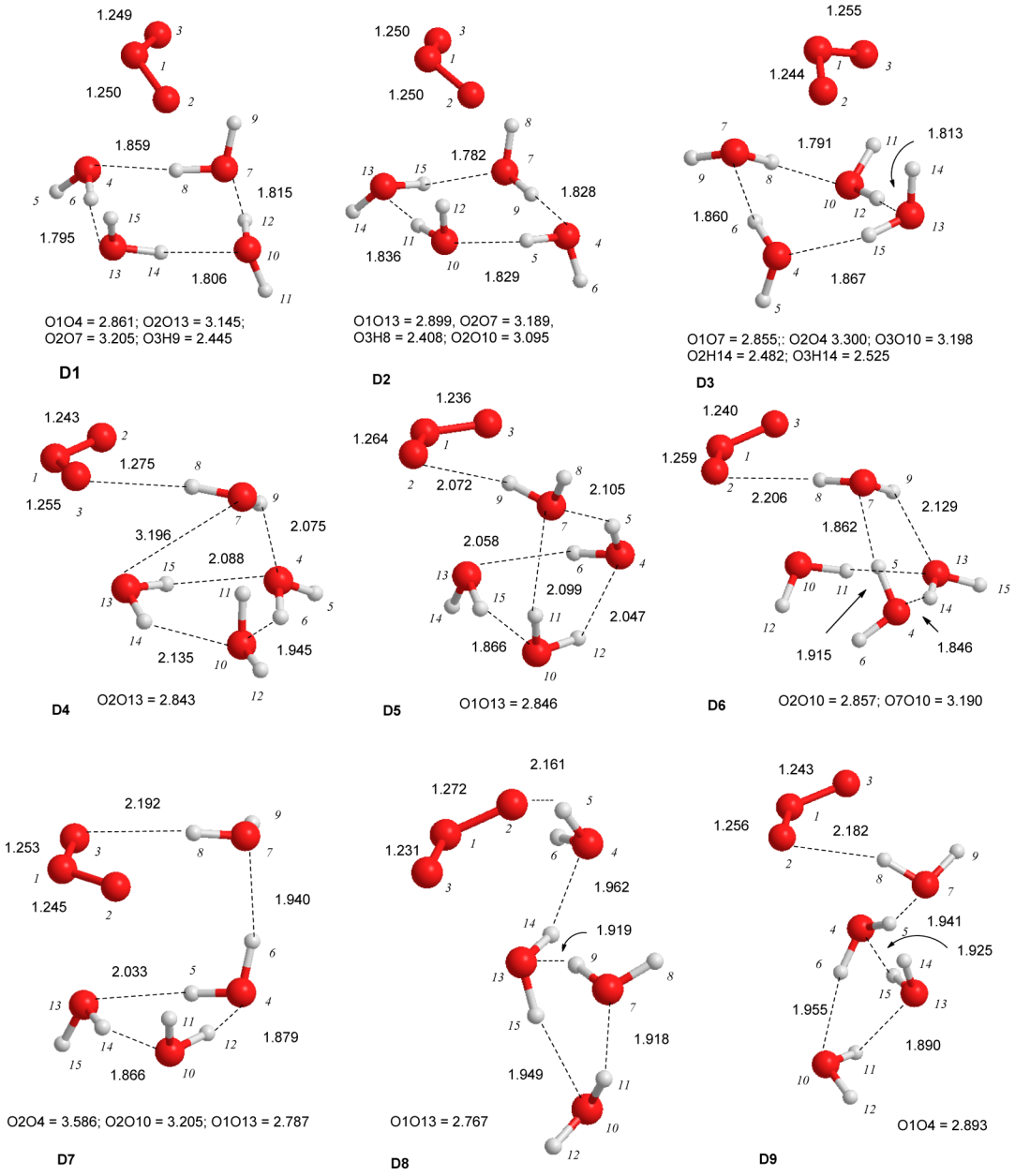

Figure 5. Relevant geometrical parameters for $O_3\cdots 4H_2O$ clusters. Distances are in Angstroms and angles in degrees. For the sake of clarity, the bond lengths of several O··O and H-bond interactions have not been explicitly drawn but written nearby each structure.

Keutsch et al.[26] The strength of these hydrogen bonds has been attributed to cooperative effects.[43,46]

Regarding the water tetramer, we report results for three different structures (see Figure 1). $(H_2O)_4$-a and $(H_2O)_4$-b have a four-membered ring structure and four hydrogen bonds, so that each water molecule acts as H-bond donor and acceptor, as in the case of the trimer. In these complexes, the four oxygen atoms almost lie in the same plane and the dangling hydrogen atoms have the *udud* and *uudd* orientation, respectively. The ring structure allows the hydrogen bonds to be quasilinear, which enhances their strength. The computed H-bond lengths range between 1.828 and 1.847 Å and are significantly shorter than those obtained for the dimer and trimer. The computed average O−O distance is 2.790 Å, similar to the value reported by Keutsch et al.[26] A closer look at the structure of these complexes indicates that they can be formed by interaction of water trimer and water molecule but also by interaction of two water dimers. Table 1 displays the computed binding energy for $(H_2O)_4$-a and $(H_2O)_4$-b that amounts 8.84 and 8.12 kcal·mol^{-1}, respectively, with respect to the $(H_2O)_3$-a + H_2O reactants and 12.98 and 12.26 kcal·mol^{-1}, respectively, with respect to the interaction of two water dimers as reactants.

The structure for $(H_2O)_4$-c differs substantially from the first two. Figure 1 shows that it can be described by the interaction of one dangling hydrogen atom of the $(H_2O)_3$-a trimer with a water monomer, so that the structure of the three-membered ring remains. Comparing the optimized geometry of this complex with that of the trimer (Figure 1) it is clearly shown that the fourth water molecule produces a significant distortion of the ring structure. Here, the extra water molecule acts as "acceptor" through the H10O9 H bond and the NBO calculation estimates a charge transfer of 9.1 me toward the three-membered ring moiety. This interaction strengthens the O8H2 hydrogen bond and simultaneously weakens the O5H7 bond (compare these

dx.doi.org/10.1021/jp407282c | J. Phys. Chem. A 2013, 117, 10381−10396

Table 2. Calculated Relative Energies, Binding Energies, Enthalpies, and Free Energies (ΔE, $\Delta(E+\mathrm{ZPE})$, $\Delta H(298\ \mathrm{K})$, and $\Delta G(298\ \mathrm{K})$, in kcal·mol^{-1}) for Formation of the Ozone−Water Complexes $O_3\cdots(H_2O)_n$ (n = 1−4)[a]

formation of $O_3\cdots H_2O$												
	$O_3 + H_2O \rightarrow O_3\cdots(H_2O)$				$O_3 + H_2O \rightarrow O_3\cdots(H_2O)$				$O_3 + H_2O \rightarrow O_3\cdots(H_2O)$			
compound	ΔE	$\Delta(E+\mathrm{ZPE})$	ΔH	ΔG	ΔE	$\Delta(E+\mathrm{ZPE})$	ΔH	ΔG	ΔE	$\Delta(E+\mathrm{ZPE})$	ΔH	ΔG
A1	−2.01	−0.94	−0.64	3.89	−2.01	−0.94	−0.64	3.89	−2.01	−0.94	−0.64	3.89
A2	−1.86	−0.76	−0.50	4.33	−1.86	−0.76	−0.50	4.33	−1.86	−0.76	−0.50	4.33
A3	−2.05	−0.76	−0.66	5.11	−2.05	−0.76	−0.66	5.11	−2.05	−0.76	−0.66	5.11
A4	−2.39	−1.27	−1.06	4.61	−2.39	−1.27	−1.06	4.61	−2.39	−1.27	−1.06	4.61
A5 (TS)	−2.27	−1.44	−1.58	4.74	−2.27	−1.44	−1.58	4.74	−2.27	−1.44	−1.58	4.74
formation of $O_3\cdots(H_2O)_2$												
	$O_3 + 2H_2O \rightarrow O_3\cdots(H_2O)_2$				$O_3 - (H_2O) + H_2O \rightarrow O_3\cdots(H_2O)_2$				$O_3 + (H_2O)_2 \rightarrow O_3\cdots(H_2O)_2$			
compound	ΔE	$\Delta(E+\mathrm{ZPE})$	ΔH	ΔG	ΔE	$\Delta(E+\mathrm{ZPE})$	ΔH	ΔG	ΔE	$\Delta(E+\mathrm{ZPE})$	ΔH	ΔG
B1	−9.62	−6.26	−6.55	8.02	−7.35	−4.82	−4.97	3.28	−4.61	−3.35	−3.22	5.42
B2	−7.32	−4.48	−4.37	8.18	−5.05	−3.04	−2.79	3.44	−2.30	−1.57	−1.04	5.58
B3	−8.87	−5.47	−5.79	8.53	−6.59	−4.03	−4.21	3.79	−3.85	−2.56	−2.46	5.93
B4	−8.88	−5.57	−5.83	8.37	−6.61	−4.13	−4.25	3.64	−3.86	−2.65	−2.50	5.77
formation of $O_3\cdots(H_2O)_3$												
	$O_3 + 3H_2O \rightarrow O_3\cdots(H_2O)_3$				$O_3 - (H_2O)_2 + H_2O \rightarrow O_3\cdots(H_2O)_3$				$O_3 + (H_2O)_3 \rightarrow O_3\cdots(H_2O)_3$			
compound	ΔE	$\Delta(E+\mathrm{ZPE})$	ΔH	ΔG	ΔE	$\Delta(E+\mathrm{ZPE})$	ΔH	ΔG	ΔE	$\Delta(E+\mathrm{ZPE})$	ΔH	ΔG
C1	−19.23	−13.07	−14.19	9.81	−9.61	−6.81	−7.64	1.79	−3.37	−2.57	−2.08	5.86
C2	−19.30	−13.15	−14.23	941	−9.68	−6.89	−7.68	1.39	−3.43	−2.65	−2.13	5.47
C3	−19.15	−12.88	−14.06	10.19	−9.53	−6.63	−7.51	2.18	−3.28	−2.38	−1.95	6.25
C4	−13.57	−8.64	−9.01	13.29	−3.95	−2.38	−2.46	5.28	2.30	1.86	3.10	9.35
formation of $O_3\cdots(H_2O)_4$												
	$O_3 + 4H_2O \rightarrow O_3\cdots(H_2O)_4$				$O_3-(H_2O)_3 + H_2O \rightarrow O_3\cdots(H_2O)_4$				$O_3 + (H_2O)_4 \rightarrow O_3\cdots(H_2O)_4$			
compound	ΔE	$\Delta(E+\mathrm{ZPE})$	ΔH	ΔG	ΔE	$\Delta(E+\mathrm{ZPE})$	ΔH	ΔG	ΔE	$\Delta(E+\mathrm{ZPE})$	ΔH	ΔG
D1	−32.01	−19.79	−22.35	12.89	−11.72	−5.65	−7.13	4.48	−3.80	−1.60	−1.38	7.71
D2	−31.89	−19.72	−22.27	13.01	−11.59	−5.58	−7.04	4.60	−3.67	−1.52	−1.30	7.83
D3	−30.77	−18.87	−21.30	13.45	−10.48	−4.73	−6.07	5.03	−2.55	−0.67	−0.32	8.27
D4	−28.46	−16.59	−19.07	16.23	−8.16	−2.45	−3.85	7.81	−0.24	1.60	1.90	11.04
D5	−26.98	−15.20	−17.60	17.60	−6.69	−1.06	−2.38	9.19	1.23	3.00	3.37	12.42
D6	−27.15	−15.90	−18.00	15.99	−6.85	−1.76	−2.77	7.58	1.07	2.30	2.98	10.81
D7	−26.82	−15.33	−17.46	16.04	−6.53	−1.19	−2.23	7.63	1.39	2.87	3.52	10.86
D8	−25.07	−13.86	−15.84	16.95	−4.78	0.28	−0.62	8.53	3.15	4.34	5.13	11.77
D9	−25.97	−14.48	−16.59	16.92	−5.68	−0.33	−1.37	8.50	2.25	3.72	4.38	11.74

[a]The ZPE and enthalpic and entropic corrections correspond to calculations at the QCISD/aug-cc-pVDZ level of theory for $O_3\cdots(H_2O)$, $O_3\cdots(H_2O)_2$, and $(H_2O)_3$ clusters and at the QCISD/6-311G(2df,2p) level of theory for the O3$\cdots(H_2O)_4$ clusters. For $O_3\cdots(H_2O)$, $O_3\cdots(H_2O)_2$, and $O_3\cdots(H_2O)_3$ the relative energies correspond to CCSD(T)/CBS//QCISD/aug-cc-pVTZ values. For $O_3\cdots(H_2O)_4$, the relative energies correspond to CCSD(T)/aug-cc-pVTZ//QCISD/aug-cc-pVDZ values.

bond lengths with the corresponding bond distances in $(H_2O)_3$-a in Figure 1). The computed incremental binding energy for this complex is 3.28 kcal·mol^{-1}, which is only 0.37 kcal·mol^{-1} larger than the binding energy of water dimer. This value, compared with the large binding energies computed for $(H_2O)_4$-a and $(H_2O)_4$-b (see Table 1), highlights the importance of cooperative effects for the last two conformers, as already pointed out in the literature.[43,46]

In addition, we carried out an extensive search of other possible stable structures of the water tetramer. Specifically, we considered the *uuud* and *uuuu* ring structures as well as two *prism* structures. In all cases we found energy minima at the QCISD/6-311G(2df,2p) level of theory but not at the QCISD/6-311+G(2df,2p) one. In this case, the calculations converged to the $(H_2O)_4$-a and $(H_2O)_4$-b minima, and therefore, we conclude that these additional structures do not exist.

In summary, the results reported in this work for the water dimer, trimer, and tetramer are in close agreement with previous theoretical results from the literature.[10,34,36−45] In general, the optimized parameters reported in the present work, obtained at the QCISD level, differ by less than 0.03 Å from the reported geometries in the literature, and our computed relative energies at CCSD(T)/CBS (for the $n(H_2O) \rightarrow (H_2O)_n$, in kcal·mol^{-1}, −5.02 for $(H_2O)_2$; −15.87 and −15.08 for $(H_2O)_3$-a and $(H_2O)_3$-b, respectively; −27.52 and −26.61 for $(H_2O)_4$-a, and $(H_2O)_4$-b, respectively) are in excellent agreement with the benchmark calculations reported recently by Temelso et al.[37] (in kcal·mol^{-1}, −5.03, −15.70, −15.08, −27.4, and −26.58 for the same species, respectively). We refer the reader to previous works for a more detailed discussion on water clusters.[10,34,36−45]

$O_3\cdots(H_2O)_n$ (n = 1−4) Complexes. The most relevant geometrical parameters for the $O_3\cdots(H_2O)_n$ (n = 1−4) complexes studied in our work are displayed in Figures 2−5 (Figure 2 also contains the results for isolated ozone). Table 2 collects the corresponding energetics. Table S1, Supporting Information, contains the topological parameters derived from the wave function. For the sake of clarity, the complexes formed by ozone with one, two, three, or four water molecules have been

dx.doi.org/10.1021/jp407282c | J. Phys. Chem. A 2013, 117, 10381−10396

labeled by prefixes A, B, C, and D, respectively. Different structures for complexes having the same number of water molecules will be distinguished by a number.

The complex formed between ozone and one water molecule has received considerable attention in the literature because it has a potential role as a possible source of hydroxyl radicals in the atmosphere[16,19,20] and also because of its possible effect on the tropospheric reactivity of ozone. This complex has been investigated by microwave, infrared, and photochemical studies[19,20,63−66] and theoretical studies as well.[64,66−73]

In the present work, we found six different stationary points involving ozone and one water molecule ($O_3\cdots H_2O$). The A1, A2, and A3 complexes are true minima and possess C_s symmetry, with all atoms lying in the molecular plane. In these complexes ozone and water are held together by one hydrogen bond involving one of the terminal oxygen atoms of ozone, and the computed binding energies are quite small at 0.94, 0.76, and 0.76 kcal·mol^{-1}, respectively (see Table 2). Not surprisingly, the length of these H bonds is quite large, between 2.23 and 2.32 Å, which are about 0.3 Å larger than the hydrogen bond of water dimer. Likewise, the NBO charge transfer and topological parameters of the wave function are smaller (q = 5.3−5.7 me; ρ = 0.0107−0.0129 au, and $\nabla^2\rho$ = 0.0412−0.0526 au, see Table S1, Supporting Information).

Structures A4, A5, and A6 do not involve H bonds, and the relative orientation of the ozone and water molecules in these complexes suggests that they are stabilized, at least in part, by dipole−dipole interactions. A4 is an asymmetric structure where the two molecules are stacked in almost parallel planes but with the water molecule slightly rotated on its symmetry axis so that the water molecule is not quite perpendicular to the axis between the central oxygen of the ozone and the oxygen in water. It has two equivalent minima on either side of a transition state with C_s symmetry; that transition state is designated A5. A swinging motion of the water molecule transforms one conformer of A4 to the other while passing through A5.

The symmetry plane of A5 contains the central oxygen atom of ozone and the oxygen atom of water and bisects the bond angles of both individual molecules. A6 also has C_s symmetry, but in this case the symmetry plane contains the three atoms of water and the central oxygen atom of ozone (the two terminal oxygen atoms of ozone being placed symmetrically to both sides of the plane of the water molecule). The frequency calculations carried out on A6 show that it has two imaginary frequencies, and any further geometry optimization starting from A6 leads to formation of A4. Hence, A6 is not a stable geometry for this complex despite its frequent appearance in the literature. Topological analysis of the wave function of A4 and A5 indicates the presence of bcp's between water and ozone oxygen atoms. For instance, in the case of A4 we found two atomic interaction lines between the terminal oxygen atoms of ozone and the oxygen atom of water (ρ_{O2O4} and ρ_{O3O4} = 0.0069 and 0.0080 au and $\nabla^2\rho_{O2O4}$ and $\nabla^2\rho_{O3O4}$ = 0.0296 and 0.0364 au as well as a ring critical point; see Table S1, Supporting Information) and a NBO charge transfer of only 1.07 me. These bcp's have the hallmark of closed shell interactions occurring in van der Waals complexes as described by Bone and Bader for the same kind of interactions.[115] Their values suggest that there is a combination of stabilization factors including polarization, dispersion, and even electron donor−acceptor (EDA) interaction in the ozone−water complex, provided the known Lewis acidity of ozone[116] and the Lewis basicity of water. The computed binding energy of A4 is 1.27 kcal·mol^{-1}, which is slightly larger than the binding energies of the H-bonded complexes (A1, A2, and A3). Regarding A5, our calculations at the best level of theory show that it lies only 0.12 kcal·mol^{-1} above A4, but when the ZPE corrections are taken into account, our results predict A5 to be 0.17 kcal·mol^{-1} more stable than A4. These results indicate a very flat potential energy surface for the swing of the water molecule over ozone so that A5 could be considered as the global thermodynamic minimum in a way similar to what occurs in some low-barrier hydrogen-bonded systems.[60,117] Thus, it turns out that *the most favorable 1:1 ozone−water complex is not a hydrogen-bonded structure but a van der Waals complex*.

As pointed out above, several theoretical studies from the literature dealt with the $O_3\cdots H_2O$ complex but the reported results strongly depend on the theoretical approach employed in the investigation (method and basis set). For instance, the MP4SDQ/6-311+G(d,p) approach predicts energy minima[68] for structures A1 and A2 and for the dipolar A6 structure. The latter is also found to be a minimum at the B3LYP level of theory.[69] The MP2/6-311++G(d,p) approach predicts A4 and A5 to be minima ,whereas A2 and the dipole stationary points are found to be transition states.[72] Finally, the CCSD/6-311++G(d,p) and QCISD/6-311++G(d,p) approaches predict A5 to be a minimum in the potential energy surface.[66,70] Interestingly, Tsuge et al.[66] predict A5 to be the only minimum for the $O_3\cdots H_2O$ complex, while the other structures correspond to transition states at the QCISD/6-311++G(d,p) level of theory. However, the results reported very recently by Kumar et al.,[73] performed at a similar theoretical level to that employed in this work, confirm that A1, A2, A3, and A4 are true minima and A5 is a transition state.

Microwave experiments by Gillies et al.[64] have suggested a dipole-like structure for the $O_3\cdots H_2O$ complex, with an average distance of 2.957 Å between the centers of mass of the two moieties (R_{cm}). Nevertheless, the angular orientation of the water unit was poorly determined. Both A5 (the global thermodynamic minimum in our study, see above) and A4 could match the predicted experimental structure, even though (a) the two hydrogen atoms do not lie in the plane perpendicular to the ozone moiety as suggested by Gillies et al.[64] and (b) the calculated values for R_{cm} are shorter than the experimental estimate (2.880 and 2.904 Åfor A4 and A5, respectively). The discrepancy between the experimental and the theoretical estimates can be understood in terms of low-frequency vibrations, as suggested by Tsuge et al.[66] Regarding the binding energies, previous QCISD(T)/6-311++G(3df,3pd) and MP4(SDQ)/6-311++G(2d,2p) approaches predict values from 2.19 to 2.39 kcal·mol^{-1},[68,72] overestimating the stability of these complexes as compared to the range from 0.76 to 1.44 kcal·mol^{-1} predicted at CCSD(T)/CBS level (see Table 2). Tsuge et al. predict a binding energy of 1.89 kcal·mol^{-1} at CCSD(T)/6-311++G(3df,3pd) including the basis set superposition error (BSSE),[66] which is more in line with our CBS results, whereas Gillies et al. predict a binding energy of 0.7 kcal·mol^{-1} at MP4(SDTQ)/6-31G(d,p), also including the BSSE correction.[64] The binding energies reported recently by Kumar et al.[73] range between 0.98 and 1.50 kcal·mol^{-1} and are in an excellent agreement with the values predicted in this work.

To the best of our knowledge, there are only three theoretical works in the literature dealing with the interaction between ozone and the water dimer, trimer, and tetramer.[69,72,73] Only one structure for each aggregate was reported in these works, and in the present study we extended the investigation by considering further clusters.

Figure 3 displays the most relevant geometrical parameters for the optimized $O_3\cdots(H_2O)_2$ complexes (B1, B2, B3, and B4). A first look at these structures shows that all of these four complexes can be directly formed either by interaction between $O_3\cdots H_2O + H_2O$ or by interaction between $O_3 + (H_2O)_2$. In all cases, the water molecules interact with each other in a way similar to what is observed in the water dimer. Indeed, topological analysis of the electron density indicates the presence of (1) a hydrogen bond between the water dimer and one of the terminal oxygen atoms of ozone and (2) a van der Waals interaction as described above for the ozone−water dimer. As a result, these complexes exhibit a three-membered ring-like structure, and topological analysis also points out the existence of a ring critical point producing a stabilization effect (see Table S1, Supporting Information). Calculated binding energies for the $O_3\cdots H_2O + H_2O \rightarrow O_3\cdots(H_2O)_2$ process range from 3.04 to 4.82 kcal·mol^{-1} (see Table 2; we considered the most stable $O_3\cdots H_2O$ complex, A3). These values are significantly smaller than the 7.55 kcal·mol^{-1} reported in the literature[69] but in good agreement with the 3.76 kcal·mol^{-1} value reported by Kumar et al.[73] For the $O_3 + (H_2O)_2 \rightarrow O_3\cdots(H_2O)_2$ process the computed binding energies range from 1.57 to 3.35 kcal·mol^{-1} (see Table 2), in line with the 3.70 kcal·mol^{-1} value reported by Loboda et al.[72]

The relative stability of these $O_3\cdots(H_2O)_2$ complexes depends on subtle differences in the interactions between the three moieties that we analyze now in some detail. For instance, the larger stability of B1 compared to B2 (1.78 kcal·mol^{-1}) can easily be explained by cooperativity effects between hydrogen bonds in the case of B1. Figure 3 shows that in both complexes the two water molecules interact with each other like in a water dimer. Then, in the case of B1, ozone interacts through an H bond with the water molecule acting as an "acceptor" regarding the water dimer moiety, which facilitates charge transfer along the two hydrogen bonds, producing a stabilizing effect. On the other side, in the case of B2, ozone interacts through an H bond with the water molecule acting as a "donor" with respect to the water dimer moiety, thus hindering charge transfer along the two hydrogen bonds and producing a destabilization effect. These facts are clearly reflected in the hydrogen-bond lengths, which are shorter in B1 (2.219 and 1.953 Å for OOO··H and HOH···OH2, respectively) than in B2 (2.640 and 2.003 Å for OOO··H and HOH···OH2, respectively). They are also reflected in the values of the density and Laplacian of the density of the corresponding hydrogen bonds (smaller in B2 than in B1) and in the computed NBO charge transfer from ozone to the water dimer moiety (7.47 me in B1 versus 2.60 me in B2, see Table S1, Supporting Information). B3 and B4 are very similar to each other and display the same hydrogen-bond pattern as in B1, although they are slightly less stable.

The EFP method agrees with QCISD in structures and relative interaction energies of $O_3\cdot\cdot(H_2O)_2$ complexes, even though the absolute values of the interaction energies are slightly more attractive (by ∼2.5 kcal·mol^{-1}), see Table 3.

The EFP results agree with NBO in characterizing bonding in B1 and B2 clusters: the polarization part of the interaction energy in B1 is −2.8 kcal·mol^{-1} versus only −1.7 kcal·mol^{-1} in B2, suggesting that the charge flow is disrupted in B2. The magnitudes of the three-body energies also suggest a similar conclusion: the three-body energy, i.e., the difference in the energy of the trimer and the energies of all dimers, is stabilizing by −0.9 kcal·mol^{-1} in B1, while the three-body energy in B2 is destabilizing by +0.2 kcal·mol^{-1}.

Table 3. Interaction Energies (kcal·mol^{-1}) for $O_3\cdots(H_2O)_2$ Clusters As Provided by the EFP Method[a]

		B1	B2	B3	B4
$O_3\cdots(H_2O)_2$	Coulomb	−13.98	−11.33	−13.56	−13.47
	Ex-Rep	10.17	7.69	9.84	9.82
	CEX	−3.82	−3.64	−3.72	−3.65
	polarization	−2.75	−1.68	−3.16	−3.19
	dispersion	−5.54	−4.60	−4.70	−4.71
	total energy	−12.10	−9.92	−11.58	−11.55
included dimers					
H_2O-H_2O	total energy	−5.61	−5.43	−5.58	−5.45
O_3-H_2O	total energy	−3.50	−3.59	−3.28	−3.03
O_3-H_2O	total energy	−2.11	−1.07	−1.63	−1.98
	two-body energy	−11.22	−10.10	−10.50	−10.47
	three-body energy	−0.88	0.18	−1.09	−1.08

[a]EFP energy components Coulomb, exchange-repulsion (Ex-Rep), polarization, and dispersion and a sum of Coulomb and exchange-repulsion terms (CEX) are also shown.

The EFP energy decomposition also provides an interesting aspect of differences in bonding between B1 and B3/B4 structures. B3 and B4 structures have higher polarization components (−3.2 kcal·mol^{-1} in B3/B4 versus −2.8 kcal·mol^{-1} in B1) but weaker dispersion (−4.7 kcal·mol^{-1} in B3 and B4 versus −5.5 kcal·mol^{-1} in B1). Thus, B3 and B4 are more polarized but have less favorable van der Waals interactions, making them overall less stable than B1. Consistent with large polarization energies, the three-body energies in B3 and B4 of 1.1 kcal·mol^{-1} are the highest among all trimers.

Interestingly, a sum of Coulomb and exchange-repulsion components in the EFP energies (which is often referred to as the first-order interaction energy) is almost constant for all trimers, from −3.6 to −3.8 kcal·mol^{-1}. Thus, the relative stability of these complexes is determined solely by higher order interactions like polarization and dispersion. This observation explains the extreme sensitivity of the ab initio results to the level of theory employed, since use of a large basis set and wave function correlation are equally important for quantitative description of the subtle balance in polarization and dispersion interactions.

Another interesting observation is that the EFP interaction energies of the water dimers computed at the geometries found in the trimers are also very similar, from −5.4 to −5.6 kcal·mol^{-1}. Thus, the relative stability of the trimers is determined by the orientation of the ozone molecule with respect to the water dimer and by the way ozone interacts with the water dimer, either building into the H-bonding network of water or maximizing van der Waals interactions with two waters. Since the trimer with the maximal dispersion interaction is the most stable structure, one might conclude that van der Waals interactions are more important in ozone−water complexes than H-bonding interactions, which is consistent with conclusions from ab initio computations.

In the case of the $O_3\cdots(H_2O)_3$ complexes, we found four different clusters, and their relevant geometrical parameters are displayed in Figure 4. In C1, C2, and C3, the three water molecules retain the ring structure of the most stable water trimer ($(H_2O)_3$-a, see above). C1 is held together by a combination of a hydrogen-bond interaction (O3···H11−O10) and van der Waals interactions, whereas C2 and C3 are pure van der Waals complexes. These three $O_3\cdots(H_2O)_3$ complexes have similar stabilities, and the binding energies range from 2.38 to 2.65 kcal·

dx.doi.org/10.1021/jp407282c | J. Phys. Chem. A 2013, 117, 10381−10396

mol^{-1} with respect to the $O_3 + (H_2O)_3 \rightarrow O_3\cdots(H_2O)_3$ process (and from 6.63 to 6.89 kcal·mol^{-1} with respect to the $O_3\cdots(H_2O)_2 + H_2O \rightarrow O_3\cdots(H_2O)_3$ process). The fourth complex (C4) displays a four-membered ring structure. It has similar geometrical features to that of the $O_3\cdots(H_2O)_2$ complexes (B1 or B3), with the third water molecule interacting with one of the dangling hydrogen atoms of water and one of the terminal oxygen atoms of ozone through two hydrogen bonds. This complex is computed to be 4.5 kcal·mol^{-1} less stable than C2 (the computed binding energy is 2.38 kcal·mol^{-1} with respect the $O_3\cdots(H_2O)_2 + H_2O \rightarrow O_3\cdots(H_2O)_3$ process).

Finally, our calculations predict the existence of up to nine clusters (D1−D9) involving ozone and four water molecules. Figure 5 shows that in three of these complexes (D1, D2, and D3) the four water molecules form a four-membered ring in a way similar to $(H_2O)_4$-a (*udud* orientation, see Figure 1). In the remaining six complexes (D4−D9) water molecules form a three-membered ring, with the fourth water molecule hydrogen bonded to it. AIM analysis of the wave function shows that in these complexes ozone is held to the water cluster through one hydrogen bond in the case of D1 and D2 and two hydrogen bonds in the case of D3, combined with van der Waals interactions between the water cluster moiety and the ozone moiety.

Figure 5 also shows that in the remaining six complexes (D4−D9) three of the water molecules form a three-membered ring structure, the fourth water is bound to the three-membered ring moiety through a hydrogen bond, and the ozone molecule is held to the cluster through one hydrogen bond between this fourth water molecule and one of the terminal oxygen atoms of O_3, along with van der Waals interactions (see Figure 5). The results displayed in Table 2 show that our calculations predict only three complexes to be stable with respect to the $O_3 + (H_2O)_4 \rightarrow O_3\cdots(H_2O)_4$ process, namely, D1, D2, and D3, having very small binding energies (between 0.67 and 1.60 kcal·mol^{-1}). Table 2 also shows that all complexes but D8 are stable with respect to $O_3\cdots(H_2O)_3 + H_2O$ ($O_3\cdots(H_2O)_3 + H_2O \rightarrow O_3\cdots(H_2O)_4$ process), and our computed binding energies range between 0.33 and 5.65 kcal·mol^{-1}. At this point it is worth mentioning that our computed binding energies for the most stable complexes are between 1 and 2 kcal·mol^{-1} smaller that the values predicted by Tachikawa et al.,[69] pointing out the importance of using large basis sets in order to obtain accurate results of binding energies for these species.

Finally, it is worth pointing out that the results reported in the present work show that the hydrogen-bond interactions between ozone and water are very weak, even weaker than van der Waals interactions between both molecules. These results are in agreement with the observed hydrophobic character of ozone.[59,61]

Equilibrium Constants and Atmospheric Concentration of the $(H_2O)_n$ and $O_3\cdots(H_2O)_n$ Clusters. In addition to the study on the stability and electronic features of the complexes investigated in this work, we calculated the corresponding equilibrium constants, which allow estimation of their atmospheric concentration. These equilibrium constants (K_{eq}) have been calculated according to eq 1

$$K_{eq} = \sigma \frac{Q_{Cluster}}{Q_{Reactan\ t1} Q_{Reactan\ t2}} e^{-(E_C - E_R)/RT} \quad (1)$$

where σ is the symmetry factor, the various Q denote the partition functions of the reactants and the cluster, and $E_C - E_R$ is the binding energy. In computing the partition functions we have taken into account the anharmonic effects by scaling the different frequencies by 0.965.[118] Figures 6 and 7 show the computed

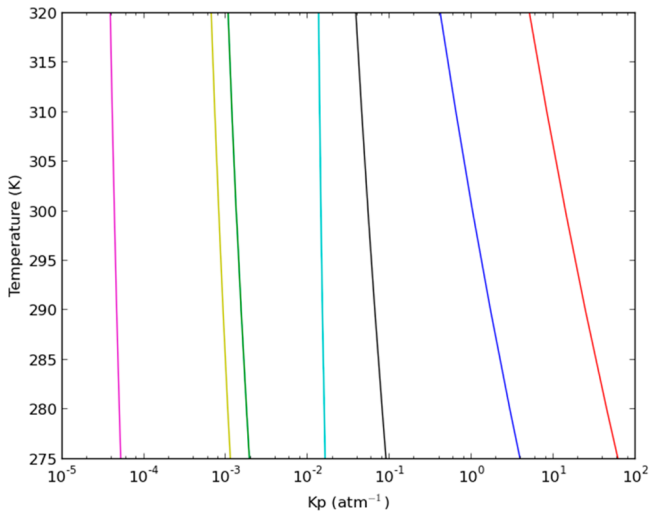

Figure 6. Equilibrium constants (K_p, in atm^{-1}) computed at different temperatures at the Earth's surface: (red) formation of $(H_2O)_4$; (blue) formation of $(H_2O)_3$; (black) formation of $(H_2O)_2$; (blue-green) formation of $O_3\cdots H_2O$; (green) formation of $O_3\cdots(H_2O)_2$; (yellow) formation of $O_3\cdots(H_2O)_3$; (magenta) formation of $O_3\cdots(H_2O)_4$.

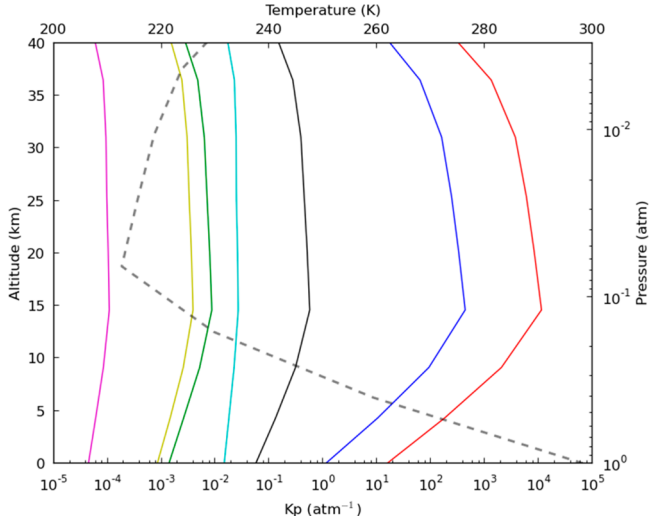

Figure 7. Calculated equilibrium constants (K_p, in atm^{-1}) as a function of the altitude of the Earth's atmosphere: (red) formation of $(H_2O)_4$; (blue) formation of $(H_2O)_3$; (black) formation of $(H_2O)_2$; (blue-green) formation of $O_3\cdot H_2O$; (green) formation of $O_3\cdots(H_2O)_2$; (yellow) formation of $O_3\cdots(H_2O)_3$; (magenta) formation of $O_3\cdots(H_2O)_4$; (dashed line) temperature in Kelvin.

equilibrium constants at different temperatures at ground level and different altitudes in the Earth atmosphere, respectively. The corresponding values are contained in Tables S2, Supporting Information.

The equilibrium constants for water clusters have been computed considering in each case the $(H_2O)_{n-1} + H_2O \rightarrow (H_2O)_n$ process. Since Keutsch and Saykally[26] have shown that the different cyclic structures are connected by transition states, for water trimer and tetramer we considered a weighted sampling of the lowest conformers (see Supporting Information). The

dx.doi.org/10.1021/jp407282c | J. Phys. Chem. A 2013, 117, 10381−10396

Table 4. Calculated Concentration of Water Clusters (in molecule·cm^{-3}) at Different Relative Humidity (RH) and Temperatures at the Ground Level of the Earth's Atmosphere

T (K)	20% RH	40% RH	60% RH	80% RH	100% RH
[H_2O]					
275.00	3.78×10^{16}	7.56×10^{16}	1.13×10^{17}	1.51×10^{17}	1.89×10^{17}
280.00	5.16×10^{16}	1.03×10^{17}	1.55×10^{17}	2.07×10^{17}	2.58×10^{17}
290.00	9.56×10^{16}	1.91×10^{17}	2.87×10^{17}	3.82×10^{17}	4.78×10^{17}
298.15	1.55×10^{17}	3.09×10^{17}	4.64×10^{17}	6.18×10^{17}	7.73×10^{17}
300.00	1.72×10^{17}	3.43×10^{17}	5.15×10^{17}	6.86×10^{17}	8.58×10^{17}
310.00	2.92×10^{17}	5.84×10^{17}	8.77×10^{17}	1.17×10^{18}	1.46×10^{18}
320.00	4.70×10^{17}	9.40×10^{17}	1.41×10^{18}	1.88×10^{18}	2.35×10^{18}
			[$(H_2O)_2$]		
275.00	4.79×10^{12}	1.92×10^{13}	4.31×10^{13}	7.67×10^{13}	1.20×10^{14}
280.00	8.18×10^{12}	3.27×10^{13}	7.36×10^{13}	1.31×10^{14}	2.04×10^{14}
290.00	2.36×10^{13}	9.46×10^{13}	2.13×10^{14}	3.78×10^{14}	5.91×10^{14}
298.15	5.44×10^{13}	2.18×10^{14}	4.90×10^{14}	8.70×10^{14}	1.36×10^{15}
300.00	6.50×10^{13}	2.60×10^{14}	5.85×10^{14}	1.04×10^{15}	1.62×10^{15}
310.00	1.63×10^{14}	6.52×10^{14}	1.47×10^{15}	2.60×10^{15}	4.06×10^{15}
320.00	3.71×10^{14}	1.48×10^{15}	3.33×10^{15}	5.92×10^{15}	9.24×10^{15}
[$(H_2O)_3$]					
275.00	2.63×10^{10}	2.10×10^{11}	7.09×10^{11}	1.68×10^{12}	3.29×10^{12}
280.00	4.69×10^{10}	3.75×10^{11}	1.27×10^{12}	3.00×10^{12}	5.85×10^{12}
290.00	1.51×10^{11}	1.21×10^{12}	4.09×10^{12}	9.68×10^{12}	1.89×10^{13}
298.15	3.83×10^{11}	3.06×10^{12}	1.03×10^{13}	2.45×10^{13}	4.78×10^{13}
300.00	4.67×10^{11}	3.73×10^{12}	1.26×10^{13}	2.98×10^{13}	5.82×10^{13}
310.00	1.29×10^{12}	1.03×10^{13}	3.47×10^{13}	8.22×10^{13}	1.60×10^{14}
320.00	3.14×10^{12}	2.51×10^{13}	8.46×10^{14}	2.00×10^{14}	3.91×10^{14}
[$(H_2O)_4$]					
275.00	2.26×10^{9}	3.62×10^{10}	1.83×10^{11}	5.79×10^{11}	1.42×10^{12}
280.00	4.09×10^{9}	6.55×10^{10}	3.31×10^{11}	1.05×10^{12}	2.55×10^{12}
290.00	1.40×10^{10}	2.23×10^{11}	1.13×10^{12}	3.57×10^{12}	8.72×10^{12}
298.15	3.68×10^{10}	5.89×10^{11}	2.98×10^{12}	9.42×10^{12}	2.30×10^{13}
300.00	4.54×10^{10}	7.26×10^{11}	3.67×10^{12}	1.16×10^{13}	2.83×10^{13}
310.00	1.30×10^{11}	2.09×10^{12}	1.06×10^{13}	3.33×10^{13}	8.11×10^{13}
320.00	3.25×10^{11}	5.19×10^{12}	2.62×10^{13}	8.29×10^{13}	2.02×10^{14}

computed K_{eq} of water dimer at room temperature is 2.28×10^{-21} cm^3·molecule^{-1}, in excellent agreement with the 1.75×10^{-21}–2.12×10^{-21} cm^3·molecule^{-1} experimental values[119−121] and also in very good agreement with previous theoretical results from the literature (ranging between 1.21×10^{-21} and 3.87×10^{-21} cm^3·molecule^{-1}).[10,11,34] For water trimer and tetramer the computed equilibrium constants are computed to be 20 and 273 times greater than that of water dimer (4.55×10^{-20} and 6.23×10^{-19} cm^3·molecule^{-1}, respectively), according to the larger relative stabilities of these complexes. Figure 6 shows that, at ground level, the equilibrium constants of the clusters diminish as the temperature increases (in the temperature range of 275−320 K). The decrease in K_{eq} is moderate for water dimer (2 times) and more pronounced (8−10 times) for water trimer and tetramer, respectively. Figure 7 shows that the value of these K_{eq}'s increases with altitude in the Earth's atmosphere, reaching a maximum at close to 15 km (with K_{eq} values of 1.63×10^{-20}, 1.24×10^{-17}, and 3.24×10^{-16} cm^3·molecule^{-1} for water dimer, trimer, and tetramer, respectively, see Table S2, Supporting Information) and then decreases in a similar way as reported in the literature.[5,11,51,122] It is also interesting to remark from Figure 7 that the changes in K_{eq} for water trimer and tetramer with respect to the altitude are very pronounced (at 15 km of altitude, the computed K_{eq} for water trimer and tetramer are 272 and 520 times larger than the corresponding values at ground level and 298 K), whereas for water dimer these changes are only moderate.

Regarding the ozone−water complexes, the equilibrium constants have been calculated for $O_3 + (H_2O)_n \rightarrow O_3\cdots(H_2O)_n$ and we considered the sum of the different $O_3\cdots(H_2O)_n$ clusters playing a role. Figures 6 and 7, and Tables S2, Supporting Information, show that at ground level and 298 K the complexes of ozone with a single water molecule have the largest equilibrium constant, followed by $O_3\cdots(H_2O)_2$, $O_3\cdots(H_2O)_3$, and $O_3\cdots(H_2O)_4$, with values of 5.91×10^{-22}, 5.55×10^{-23}, 3.38×10^{-23}, and 1.78×10^{-24} cm^3·molecule^{-1}, respectively. This order contrasts with the order on the binding energies (3.35 kcal·mol^{-1} for complex B1 of $O_3\cdots(H_2O)_2$; 2.65 kcal·mol^{-1} for complex C2 of $O_3\cdots(H_2O)_3$; 1.60 kcal·mol^{-1} for complex D1 of $O_3\cdots(H_2O)_4$; and 1.27 kcal·mol^{-1} for complex A5 of $O_3\cdots H_2O$ (see Table 2) and underscores the importance of differential entropic effects as reflected in the ΔG values of Table 2. Figures 6 and 7 also show that the equilibrium constants of the ozone−water complexes follow similar trends to the water clusters with respect to temperature and altitude in the Earth's atmosphere, as discussed above. Our calculations predict that, at ground level, the values of K_{eq} in the 275−320 K range of temperatures for these ozone−water complexes remain almost constant, whereas with respect to the altitude in the Earth's atmosphere, our results predict a very smooth increase in K_{eq} up to 15 km and then a very slight decrease, in line with the results reported in the literature.[5]

dx.doi.org/10.1021/jp407282c | J. Phys. Chem. A 2013, 117, 10381−10396

Table 5. Calculated Concentration of Water Clusters (in molecule·cm^{-3}) at Different Altitudes in the Earth's Atmosphere[a]

altitude (km)	T (K)	P (atm)	$[H_2O]$	$[(H_2O)_2]$	$[(H_2O)_3]$	$[(H_2O)_4]$
0	298.15	1.000	7.37×10^{17}	1.24×10^{15}	5.15×10^{13}	1.90×10^{13}
5	259.30	0.535	2.41×10^{16}	2.67×10^{12}	2.32×10^{10}	3.52×10^{9}
10	229.70	0.266	4.92×10^{15}	2.31×10^{11}	3.25×10^{9}	1.01×10^{9}
15	212.60	0.120	1.96×10^{13}	6.26×10^{6}	1.52×10^{3}	9.66
20	215.50	0.054	9.56×10^{12}	1.35×10^{6}	1.24×10^{2}	
25	218.60	0.025	5.21×10^{12}	3.58×10^{5}	1.33×10^{1}	
30	223.70	0.011	2.62×10^{12}	8.03×10^{4}	1.01	
35	235.10	0.005	1.31×10^{12}	1.50×10^{4}		
40	249.90	0.003	6.44×10^{12}	2.12×10^{5}		

[a] T and P values and water vapor concentrations are taken form ref 16.

Table 6. Calculated Concentration of $O_3\cdots(H_2O)_n$ Clusters (in molecule·cm^{-3}) at Different Relative Humidity (RH) and Temperatures at the Ground Level of the Earth's Atmosphere[a]

T	20 RH	40 RH	60 RH	80 RH	100 RH
			$[O_3\cdots H_2O]$		
275.00	9.53×10^{6}	1.91×10^{7}	2.85×10^{7}	3.81×10^{7}	4.76×10^{7}
280.00	1.29×10^{7}	2.58×10^{7}	3.88×10^{7}	5.18×10^{7}	6.46×10^{7}
290.00	2.37×10^{7}	4.73×10^{7}	7.10×10^{7}	9.46×10^{7}	1.18×10^{8}
298.15	3.81×10^{7}	7.60×10^{7}	1.14×10^{8}	1.52×10^{8}	1.90×10^{8}
300.00	4.23×10^{7}	8.43×10^{7}	1.27×10^{8}	1.69×10^{8}	2.11×10^{8}
310.00	7.14×10^{7}	1.43×10^{8}	2.15×10^{8}	2.86×10^{8}	3.57×10^{8}
320.00	1.15×10^{8}	2.30×10^{8}	3.44×10^{8}	4.59×10^{8}	5.74×10^{8}
			$[O_3\cdots(H_2O)_2]$		
275.00	1.44×10^{2}	5.77×10^{2}	1.29×10^{3}	2.30×10^{3}	3.60×10^{3}
280.00	2.31×10^{2}	9.22×10^{2}	2.08×10^{3}	3.69×10^{3}	5.75×10^{3}
290.00	5.94×10^{3}	2.38×10^{3}	5.36×10^{3}	9.51×10^{3}	1.49×10^{4}
298.15	1.26×10^{3}	5.03×10^{3}	1.13×10^{4}	2.01×10^{4}	3.14×10^{4}
300.00	1.48×10^{3}	5.91×10^{3}	1.33×10^{4}	2.36×10^{4}	3.68×10^{4}
310.00	3.38×10^{3}	1.35×10^{4}	3.05×10^{4}	5.39×10^{4}	8.41×10^{4}
320.00	7.10×10^{3}	2.83×10^{4}	6.37×10^{4}	1.13×10^{5}	1.77×10^{5}
			$[O_3\cdots(H_2O)_3]$		
275.00		3.69	1.24×10^{1}	2.95×10^{1}	5.78×10^{1}
280.00		6.24	2.11×10^{1}	4.99×10^{1}	9.73×10^{2}
290.00	2.28	1.83×10^{1}	6.18×10^{1}	1.46×10^{2}	2.85×10^{2}
298.15	5.39	4.30×10^{1}	1.45×10^{2}	3.44×10^{2}	6.72×10^{2}
300.00	6.47	5.17×10^{1}	1.75×10^{2}	4.13×10^{2}	8.06×10^{2}
310.00	1.66×10^{1}	1.32×10^{2}	4.46×10^{2}	1.06×10^{3}	2.06×10^{3}
320.00	3.76×10^{1}	3.01×10^{2}	1.01×10^{3}	2.40×10^{3}	4.68×10^{3}

[a] These values have been computed taking the water cluster concentrations of Table 4 and the ozone concentration of 4.16×10^{-11} molecule·cm^{-3} (taken from ref 16). The concentration of $O_3\cdots(H_2O)_4$ clusters is negligible.

An important issue for atmospheric purposes is to estimate the atmospheric concentration of the $(H_2O)_n$ and $O_3\cdots(H_2O)_n$ (n = 1−4) complexes, which can be done by taking the equilibrium constants reported in this work. Tables 4−7 contain the calculated concentrations of these clusters, computed at different conditions of temperature and relative humidity (RH) at ground level and at different altitudes of the Earth atmosphere. The concentrations of these clusters depend on the concentration of water vapor and ozone.

For the Earth's surface we considered water vapor concentrations between 20% and 100% of RH in the 273−320 K temperature range and estimate the concentration of water dimers to be between 4.79×10^{12} molecules·cm^{-3} at 273 K and 20% of RH and 9.24×10^{15} molecules·cm^{-3} at 320 K and 100% of RH (see Table 4). The concentration of water trimers ranges between 2.63×10^{10} and 3.91×10^{14} molecules·cm^{-3}, and for water tetramers we estimate concentrations ranging from 2.26×10^{9} to 2.02×10^{14} molecules·cm^{-3}, in the same interval of temperatures and RH (see Table 4). For water dimers, our values compare quite well with values previously reported in the literature, ranging from 5.95×10^{13} to 1.7×10^{15} molecules·cm^{-3}.[10,34,119,123] According to the results in Table 5, our calculations predict significant concentrations of water clusters up to a high of 10 km (2.31×10^{11}, 3.25×10^{9}, and 1.01×10^{9} molecules·cm^{-3} for water dimer, trimer, and tetramer, respectively). At higher altitudes the dimer concentration drops significantly and the trimers and tetramers are negligible.

In order to estimate the atmospheric abundances of ozone−water clusters we considered the density numbers of water clusters from Tables 4 and 5 and ozone concentrations taken from ref 16, namely, 4.16×10^{11} molecules·cm^{-3} at ground level and values ranging from 4.16×10^{11} to 8.21×10^{12} molecules·cm^{-3} at different altitudes in the Earth atmosphere. Our calculations predict that, at ground level, the concentration of $O_3\cdots H_2O$ clusters ranges from 9.53×10^{6} molecules·cm^{-3} at 280 K and 20% of RH to 5.74×10^{8} molecules·cm^{-3} at 320 K and

dx.doi.org/10.1021/jp407282c | J. Phys. Chem. A 2013, 117, 10381−10396

Table 7. Calculated Concentration of $O_3\cdots(H_2O)_n$ Clusters (in molecule·cm^{-3}) at Different Altitudes in the Earth's Atmosphere[a]

altitude (km)	T (K)	P (atm)	$[O_3]$	$[O_3\cdots H_2O]$	$[O_3\cdots(H_2O)_2]$
0	298.15	1.000	4.16×10^{11}	1.81×10^{8}	2.86×10^{4}
5	259.30	0.535	4.62×10^{11}	6.96×10^{6}	1.12×10^{2}
10	229.70	0.266	4.57×10^{12}	1.56×10^{7}	1.68×10^{2}
15	212.60	0.120	1.32×10^{12}	1.98×10^{4}	
20	215.50	0.054	2.93×10^{12}	2.11×10^{4}	
25	218.60	0.025	2.96×10^{12}	1.12×10^{4}	
30	223.70	0.011	1.85×10^{12}	3.56×10^{3}	
35	235.10	0.005	8.21×10^{12}	7.71×10^{3}	
40	249.90	0.003	2.37×10^{11}	8.82×10^{2}	

[a] T and P values and ozone concentrations are taken form ref 16. Concentration of water clusters displayed in Table 5 is employed. Concentrations of $O_3\cdots(H_2O)_3$ and $O_3\cdots(H_2O)_4$ complexes are negligible.

100% of RH, which are around 1 order of magnitude larger than the values estimated by Frost and Vaida[16] (ranging between 1.96×10^6 and 3.7×10^7 molecules·cm^{-3}).

The computed concentrations of $O_3\cdots(H_2O)_2$ and $O_3\cdots(H_2O)_3$ are much smaller, with values up to only 1.77×10^5 and 4.68×10^3 molecules·cm^{-3}, respectively, in very hot and humid conditions (at 320 K and 100% of RH, see Table 6). The $O_3\cdots(H_2O)_4$ complexes will not have any significance. Calculated concentrations of ozone–water clusters at different altitudes in the Earth's atmosphere are displayed in Table 7, which shows that only the $O_3\cdots H_2O$ clusters will have some importance up to 10 km of altitude of the Earth's atmosphere (with predicted concentrations of 6.96×10^6 and 1.56×10^7 molecules·cm^{-3} at 5 and 10 km, respectively), but at higher altitudes its concentration drops off very rapidly. Our results predict concentrations of $O_3\cdots H_2O$ clusters between 1 and 2 orders of magnitude larger than the values reported by Frost and Vaida (for instance, between 3.03×10^4 and 8.56×10^5 molecules·cm^{-3} at 5 km of altitude and between 4.85×10^3 and 2.05×10^5 molecules·cm^{-3} at 10 km of altitude).[16]

Finally, it is worth pointing out at this point that the accuracy of our results can be estimated comparing our calculated values with the experimental ones for water dimer, which has been extensively discussed above. In this case our binding energy differs from the experimental value in 0.3–0.5 kcal/mol only and the equilibrium constant between 1.08 and 1.3 times. Provided that all complexes but $O_3\cdots(H_2O)_4$ are computed at the same level of theory, namely, CCSD(T)/CBS, we expect similar accuracy. The energy of $O_3\cdots(H_2O)_4$ complexes has been computed at the CCSD(T)/aug-cc-pVTZ level only, and for these complexes, we expect less accuracy in our results of about 1 kcal/mol in the binding energy and a factor of about 4–5 times in the equilibirum constant.

CONCLUSIONS

In this work we performed an exhaustive investigation of water clusters $(H_2O)_n$, n = 1–4, and the complexes formed between these water clusters and one ozone molecule. We employed high-level theoretical methods and highlight the following points.

We considered the water dimer, the two cyclic structures of water trimer, and three water tetramer complexes. Two of them have a ring structure, and the third one involves the interaction of water trimer with a dangling water molecule. An extensive search for additional $(H_2O)_4$ structures having either a four-membered ring or prism structure, at the QCISD level of theory, has failed, and we conclude that these structures do not exist. The computed incremental binding energies for the most stable complexes of water dimer, trimer, and tetramer are 2.91, 7.59, and 8.84 kcal·mol^{-1}, respectively.

The most stable complex involving ozone and one water molecule is held together by van der Waals interactions, whereas the $O_3\cdots(H_2O)_n$ (n = 2–4) complexes are held together by a combination of van der Waals and hydrogen-bond interactions. The incremental binding energies of these complexes are predicted to be very small, ranging between 0.67 and 3.34 kcal·mol^{-1}.

A very interesting finding from our investigation is that the hydrogen-bond strengths between ozone and water are very weak, even weaker than the van der Waals interactions between both molecules, and these results *are in agreement with the observed hydrophobic character of ozone.*

Regarding water clusters, our calculations allow estimation of the concentration of the complexes investigated in this work at different conditions in the Earth's atmosphere. The density numbers for water dimer range from 4.79×10^{12} molecule·cm^{-3} in very cold and dry conditions to 9.24×10^{15} molecule·cm^{-3} in very hot and humid conditions and are in good agreement with experimental estimates. The concentrations of water trimer and tetramer range from 2.63×10^{10} to 3.91×10^{14} and from 2.26×10^9 to 2.02×10^{14} molecule·cm^{-3}, respectively, in the same conditions. The concentration of these species may be relevant up to 10 km of altitude in the Earth's atmosphere (2.31×10^{11}, 3.25×10^9, and 1.01×10^9 molecule·cm^{-3}, respectively) and drop off very quickly at higher altitudes.

Our calculations predict the concentration of $O_3\cdots H_2O$ complex to be between 1 and 2 orders of magnitude larger than previously estimated in the literature, up to 5.74×10^8 molecules·cm^{-3} under very hot and humid conditions at ground level and 1.56×10^7 molecules·cm^{-3} at 10 km of altitude of the Earth atmosphere. This is important provided that photolysis of this complex constitutes an additional source of hydroxyl radical in the atmosphere. The predicted concentrations of $O_3\cdots(H_2O)_2$ and $O_3\cdots(H_2O)_3$ are very small at ground level and negligible at different altitudes in the atmosphere. $O_3\cdots(H_2O)_4$ will not exist in the atmosphere.

ASSOCIATED CONTENT

Supporting Information

Tables with results of AIM analysis, rate constants computed under different conditions of temperature and pressure, absolute energies, and Cartesian coordinates of all structures investigated in this work. This material is available free of charge via the Internet at http://pubs.acs.org.

AUTHOR INFORMATION

Corresponding Authors

*E-mail: anglada@iqac.csic.es.
*E-mail: francisc@purdue.edu

Notes

The authors declare no competing financial interest.

ACKNOWLEDGMENTS

This work was supported by the Spanish DGYCIT (CTQ2011-27812) and the Generalitat de Catalunya (Grant 2009SGR01472). Calculations described in this work were

carried out at the Centre de Supercomputació de Catalunya (CESCA) and at CTI-CSIC, except for the Monte Carlo searches and preliminary MP2 optimizations, which were carried out at the Research Computing facility (RCAC) at Purdue University. G.J.H. thanks Edinboro University of Pennsylvania for its grant of sabbatical leave. L.V.S. acknowledges support of Purdue University.

REFERENCES

(1) Stockwell, W. R.; Lawson, C. V.; Saunders, E.; Goliff, W. S. A Review of Tropospheric Atmospheric Chemistry and Gas-Phase Chemical Mechanisms for Air Quality Modeling. *Atmosphere* **2012**, *3*, 1−32.

(2) Buszek, R. J.; Francisco, J. S.; Anglada, J. M. Water Effects on Atmospheric Reactions. *Int. Rev. Phys. Chem.* **2011**, *30*, 335−369.

(3) Sennikov, P. G.; Ignatov, S. K.; Schrems, O. Complexes and Clusters of Water Relevant to Atmospheric Chemistry: H_2O Complexes with Oxidants. *ChemPhysChem* **2005**, *6*, 392−412.

(4) Staikova, M.; Donaldson, D. J. Water Complexes as Catalysts in Atmospheric Reactions. *Phys. Chem. Earth, Part C: Sol., Terr. Planet. Sci.* **2001**, *26*, 473−478.

(5) Vaida, V.; Kjaergaard, H. G.; Feierabend, K. J. Hydrated Complexes: Relevance to Atmospheric Chemistry and Climate. *Int. Rev. Phys. Chem.* **2003**, *22*, 203−219.

(6) Vaida, V. Perspective: Water Cluster Cediated Atmospheric Chemistry. *J. Chem. Phys.* **2011**, *135*, 020901.

(7) Anglada, J. M.; Gonzalez, J.; Torrent-Sucarrat, M. Effects of the Substituents on the Reactivity of Carbonyl Oxides. A Theoretical Study on the Reaction of Substituted Carbonyl Oxides with Water. *Phys. Chem. Chem. Phys.* **2011**, *13*, 13034−13045.

(8) Vaida, V.; Daniel, J. S.; Kjaergaard, H. G.; Goss, L. M.; Tuck, A. F. Atmospheric Absorption of near Infrared and Visible Solar Radiation by the Hydrogen Bonded Water Dimer. *Q. J. R. Meteorolog. Soc* **2001**, *127*, 1627−1643.

(9) Anglada, J. M.; Gonzalez, J. Different Catalytic Effects of a Single Water Molecule: The Gas-Phase Reaction of Formic Acid with Hydroxyl Radical in Water Vapor. *ChemPhysChem* **2009**, *10*, 3034−3045.

(10) Gonzalez, J.; Caballero, M.; Aguilar-Mogas, A.; Torrent-Sucarrat, M.; Crehuet, R.; Solé, A.; Giménez, X.; Olivella, S.; Bofill, J.; Anglada, J. The Reaction Between HO and $(H_2O)_n$; (n = 1, 3) Clusters: Reaction Mechanisms and Tunneling Effects. *Theor. Chem. Acc.* **2011**, *128*, 579−592.

(11) Torrent-Sucarrat, M.; Francisco, J. S.; Anglada, J. M. Sulfuric Acid as Autocatalyst in the Formation of Sulfuric Acid. *J. Am. Chem. Soc.* **2012**, *134*, 20632−20644.

(12) Jorgensen, S.; Kjaergaard, H. G. Effect of Hydration on the Hydrogen Abstraction Reaction by HO in DMS and its Oxidation Products. *J. Phys. Chem. A* **2010**, *114*, 4857−4863.

(13) Thomsen, D. L.; Kurten, T.; Jorgensen, S.; Wallington, T. J.; Baggesen, S. B.; Aalling, C.; Kjaergaard, H. G. On the Possible Catalysis by Single Water Molecules of Gas-Phase Hydrogen Abstraction Reactions by OH radicals. *Phys. Chem. Chem. Phys.* **2012**, *14*, 12992−12999.

(14) Morrell, T. E.; Shields, G. C. Atmospheric Implications for Formation of Clusters of Ammonium and 1−10 Water Molecules. *J. Phys. Chem. A* **2010**, *114*, 4266−4271.

(15) Jorgensen, S.; Jensen, C.; Kjaergaard, H. G.; Anglada, J. M. The Gas-Phase Reaction of Methane Sulfonic Acid with the Hydroxyl Radical without and with Water Vapor. *Phys. Chem. Chem. Phys.* **2013**, *15*, 5140−5150.

(16) Frost, G.; Vaida, V. Atmospheric Implications of the Photolysis of the Ozone−Water Weakly-Bound Complex. *J. Geophys. Res. Atmos.* **1995**, *100* (D9), 18803−18809.

(17) Vaida, V.; Kjaergaard, H. G.; Hintze, P. E.; Donaldson, D. J. Photolysis of Sulfuric Acid Vapor by Visible Solar Radiation. *Science* **2003**, *299*, 1566−1568.

(18) Vaida, V.; Donaldson, D. J.; Strickler, S. J.; Stephens, S. L.; Birks, J. W. A Reinvestigation of the Electronic-spectra of Ozone-Codensed Phase Effects. *J. Phys. Chem.* **1989**, *93*, 506−508.

(19) Buckley, P. T.; Birks, J. W. Evaluation of Visible-Light Photolysis of Ozone−Water Cluster Molecules as a Source of Atmospheric Hydroxyl Radical and Hydrogen Peroxide. *Atmos. Environ.* **1995**, *29*, 2409−2415.

(20) Jin, B.; Su, M.-N.; Lin, J. J.-M. Does Ozone−Water Complex Produce Additional OH Radicals in the Atmosphere? *J. Phys. Chem. A* **2012**, *116*, 12082−12088.

(21) Nelander, B. Matrix-Isolation Studies of Water Complexes. *J. Mol. Struct.* **1990**, *222*, 121−126.

(22) Ceponkus, J.; Uvdal, P.; Nelander, B. Water Tetramer, Pentamer, and Hexamer in Inert Matrices. *J. Phys. Chem. A* **2012**, *116*, 4842−4850.

(23) Pugliano, N.; Saykally, R. J. Measurements of Quantum Tunneling Between Chiral Isomers of the Cyclic Water Trimer. *Science* **1992**, *257*, 1937−1940.

(24) Paul, J. B.; Collier, C. P.; Saykally, R. J.; Scherer, J. J.; Okeefe, A. Direct Measurement of Water Cluster Concentrations by Infrared Cavity Ringdown Laser Absorption Spectroscopy. *J. Phys. Chem. A* **1997**, *101*, 5211−5214.

(25) Ludwig, R. Water: From Custers to the Bulk. *Angew. Chem., Int. Ed.* **2001**, *40*, 1808−1827.

(26) Keutsch, F. N.; Saykally, R. J. Water clusters: Untangling the Mysteries of the Liquid, one Molecule at a Time. *Proc. Natl. Acad. Sci.* **2001**, *98*, 10533−10540.

(27) Keutsch, F. N.; Cruzan, J. D.; Saykally, R. J. The Water Trimer. *Chem. Rev.* **2003**, *103*, 2533−2577.

(28) Rocher-Casterline, B. E.; Ch'ng, L. C.; Mollner, A. K.; Reisler, H. Communication: Determination of the Bond Dissociation Energy (D-0) of the Water Dimer, $(H_2O)_2$, by Velocity Map Imaging. *J. Chem. Phys.* **2011**, *134*, 211101.

(29) Curtiss, L. A.; Frurip, D. J.; Blander, M. Studies of Molecular Association in H_2O and D_2O Vapors by Measurements of Thermal-Conductivity. *J. Chem. Phys.* **1979**, *71*, 2703−2711.

(30) Bondarenko, G. V.; Gorbaty, Y. E. An Infrared Study of Water-Vapor in the Temperature Range 573−723-K - Dimerization Enthalpy and Absorption Intensities for Monomer and Dimer. *Mol. Phys.* **1991**, *74*, 639−647.

(31) Jin, Y. S.; Ikawa, S. Near-Infrared Spectroscopic Study of Water at High Temperatures and Pressures. *J. Chem. Phys.* **2003**, *119*, 12432−12438.

(32) Nakayama, T.; Fukuda, H.; Kamikawa, T.; Sakamoto, Y.; Sugita, A.; Kawasaki, M.; Amano, T.; Sato, H.; Sakaki, S.; Morino, I.; Inoue, G. Effective Interaction Energy of Water Dimer at Room Temperature: An Experimental and Theoretical Study. *J. Chem. Phys.* **2007**, *127*, 134302.

(33) Klopper, W.; van Duijneveldt-van de Rijdt, J.; van Duijneveldt, F. B. Computational Determination of Equilibrium Geometry and Dissociation Energy of the Water Dimer. *Phys. Chem. Chem. Phys.* **2000**, *2*, 2227−2234.

(34) Dunn, M. E.; Pokon, E. K.; Shields, G. C. Thermodynamics of Forming Water Clusters at Various Temperatures and Pressures by Gaussian-2, Gaussian-3, Complete Basis Set-QB3, and Complete Basis Set-APNO Model Chemistries; Implications for Atmospheric Chemistry. *J. Am. Chem. Soc.* **2004**, *126*, 2647−2653.

(35) Shank, A.; Wang, Y.; Kaledin, A.; Braams, B. J.; Bowman, J. M. Accurate Ab Initio and "Hybrid" Potential Energy Surfaces, Intramolecular Vibrational Energies, and Classical IR Spectrum of the Water Dimer. *J. Chem. Phys.* **2009**, *130*, 144314.

(36) Shields, R. M.; Temelso, B.; Archer, K. A.; Morrell, T. E.; Shields, G. C. Accurate Predictions of Water Cluster Formation, $(H_2O)_n$ (n = 2−10). *J. Phys. Chem. A* **2010**, *114*, 11725−11737.

(37) Temelso, B.; Archer, K. A.; Shields, G. C. Benchmark Structures and Binding Energies of Small Water Clusters with Anharmonicity Corrections. *J. Phys. Chem. A* **2011**, *115*, 12034−12046.

(38) Xantheas, S. S.; Dunning, T. H. The Structure of the Water Trimer from Ab Initio Calculations. *J. Chem. Phys.* **1993**, *98* (10), 8037−8040.

(39) Xantheas, S. S.; Dunning, T. H. Ab Initio Studies of Cyclic Water Clusters $(H_2O)_n$, n = 1−6.1. Optimal Structures and Vibrational Spectra. *J. Chem. Phys.* **1993**, *99*, 8774−8792.
(40) Xantheas, S. S.; Burnham, C. J.; Harrison, R. J. Development of Transferable Interaction Models for Water. II. Accurate Energetics of the First Few Water Clusters from First Principle. *J. Chem. Phys.* **2002**, *116*, 1943.
(41) Loboda, O. A.; Goncharuk, V. V. Ab Initio Calculations of Water Clusters. The Vibratory Analysis and Isotopic Effect. *J. Water Chem. Technol.* **2009**, *31*, 98−109.
(42) Qian, P.; Song, W.; Lu, L.; Yang, Z. Ab Initio Investigation of Water Clusters $(H_2O)(n)$ (n = 2−34). *Int. J. Quantum Chem.* **2010**, *110*, 1923−1937.
(43) Cobar, E. A.; Horn, P. R.; Bergman, R. G.; Head-Gordon, M. Examination of the Hydrogen-Bonding Networks in Small Water Clusters (n = 2−5, 13, 17) Using Absolutely Localized Molecular Orbital Energy Decomposition Analysis. *Phys. Chem. Chem. Phys.* **2012**, *14*, 15328−15339.
(44) Gillan, M. J.; Manby, F. R.; Towler, M. D.; Alfè, D. Assissing the Accuracy of Quantum Monte Carlo and Density Functional Theory for Energetics of Small Water Clusters. *J. Chem. Phys.* **2012**, *136*, 244105.
(45) Klopper, W.; Schutz, M.; Luthi, H. P.; Leutwyler, S. J. An Ab-Initio Derived Torsional Potential-Energy Surface for $(H_2O)_3$. 2. Benchmark Studies and Interaction Energies. *J. Chem. Phys.* **1995**, *103*, 1085.
(46) Xantheas, S. S. Cooperativity and Hydrogen Bonding Network in Water Clusters. *Chem. Phys.* **2000**, *258*, 225−231.
(47) Daniel, J. S.; Solomon, S.; Kjaergaard, H. G.; et al. Atmospheric Water Vapor Complexes and the Continuum. *Geophys. Res. Lett.* **2004**, *31*, L06118.
(48) Salmi, T.; HÃnninen, V.; Garden, A. L.; Kjaergaard, H. G.; Tennyson, J.; Halonen, L. Correction to the Calculation of the O−H Stretching Vibrational Overtone Spectrum of the Water Dimer. *J. Phys. Chem. A* **2012**, *116*, 796−797.
(49) Garden, A. L.; Halonen, L.; Kjaergaard, H. G. Widening of the Hydrogen Bonded OH-Streching Bands Due to the Wagging and OO-Stretching Modes in $H_2O{\cdot}H_2O$. *Chem. Phys. Lett.* **2011**, *513*, 167−172.
(50) Garden, A. L.; Halonen, L.; Kjaergaard, H. G. Calculated Band Profiles of the OH-Stretching Transitions in Water Dimer. *J. Phys. Chem. A* **2008**, *112*, 7439−7447.
(51) Headrick, J. E.; Vaida, V. Significance of Water Complexes in the Atmosphere. *Phys. Chem. Earth, Part C: Sol. Terr. Planet. Sci.* **2001**, *26*, 479−486.
(52) Daniel, J. S.; Solomon, S.; Kjaergaard, H. G.; Schofield, D. P. Atmospheric Water Vapor Complexes and the Continuum. *Geophys. Res. Lett.* **2004**, *31*, L06118.
(53) Schenter, G. K.; Kathmann, S. M.; Garrett, B. C. Dynamical Nucleation Theory: A New Molecular Approach to Vapor-Liquid Nucleation. *Phys. Rev. Lett.* **1999**, *82*, 3484−3487.
(54) Morokuma, K.; Muguruma, C. Ab Initio Molecular Orbital Study of the Mechanism of the Gas Phase Reaction $SO_3 + H_2O$: Importance of the Second Water Molecule. *J. Am. Chem. Soc.* **1994**, *116*, 10316−10317.
(55) Kolb, C. E.; Jayne, J. T.; Worsnop, D. R.; Molina, M. J.; Meads, R. F.; Viggiano, A. A. Gas-Phase Reaction of Sulfur-Trioxide with Water-Vapor. *J. Am. Chem. Soc.* **1994**, *116*, 10314−10315.
(56) Gebbie, H. A.; Burrough, Wj; Chamberl, J.; Harries, J. E.; Jones, R. G. Dimers of Water Molecule in the Earth's Atmosphere. *Nature* **1969**, *221* (5176), 143−145.
(57) Tretyakov, M. Y.; Serov, E. A.; Koshelev, M. A.; Parshin, V. V.; Krupnov, A. F. Water Dimer Rotationally Resolved Millimeter-Wave Spectrum Observation at Room Temperature. *Phys. Rev. Lett.* **2013**, *110*, 093001.
(58) Finlayson-Pitts., B.; J. Pitts, J. *Chemistry of the Upper and Lower Atmosphere. Theory, Experiments, and Applications*; Academic Press: San Diego, 2000.
(59) Chalmet, S.; Ruiz-López, M. F. The Structure of Ozone and HO_x Radicals in Aqueous Solution from Combined Quantum/Classical Molecular Dynamics Simulations. *J. Chem. Phys.* **2006**, *124*, 194502.
(60) Anglada, J. M.; Torrent-Sucarrat, M.; Ruiz-Lopez, M. F.; Martins-Costa, M. Is the HO_4^-Anion a Key Species in the Aqueous-Phase Decomposition of Ozone? *Chem. Eur. J.* **2012**, *18*, 13435−13445.
(61) Vacha, R.; Slavicek, P.; Mucha, M.; Finlayson-Pitts, B. J.; Jungwirth, P. Adsorption of Atmospherically Relevant Gases at the Air/Water Interface: Free Energy Profiles of Aqueous Solvation of N_2, O_2, O_3, OH, H_2O, HO_2, and H_2O_2. *J. Phys. Chem. A* **2004**, *108*, 11573−11579.
(62) Donaldson, D. J.; Valsaraj, K. T. Adsorption and Reaction of Trace Gas-Phase Organic Compounds on Atmospheric Water Film Surfaces: A Critical Review. *Environ. Sci. Technol.* **2010**, *44*, 865−873.
(63) Schriver, L.; Barreau, C.; Schriver, A. Infrared Spectroscopic and Photochemical Study of Water-Ozone Complexes in Solid Argon. *Chem. Phys.* **1990**, *140*, 429−438.
(64) Gillies, J. Z.; Gillies, C. W.; Suenram, R. D.; Lovas, F. J.; Schmidt, T.; Cremer, D. A A Microwave Specteal and Ab Initio Investigation of O_3-H_2O. *J. Mol. Spectrosc.* **1991**, *146*, 493−512.
(65) King, D. S.; Sauder, D. G.; Casassa, M. P. Cluster Effects in O_3/H_2O Photochemistry -Dynamics of the O+H_2O- 2OH Reaction Photoinitiated in the $O_3{\cdot}$ H_2O Dimer. *J. Chem. Phys.* **1994**, *100*, 4200−4210.
(66) Tsuge, M.; Tsuji, K.; Kawai, A.; Shibuya, K. Infrared Spectroscopy of Ozone−Water Complex in a Neon Matrix. *J. Phys. Chem. A* **2007**, *111*, 3540−3547.
(67) Zakharov, I. I.; Kolbasina, O. I.; Semenyuk, T. N.; Tyupalo, N. F.; Zhidomirov, G. M. Molecular Ozone−Water Complex. Ab Initio Calculation with Inculsion of the Electron Correlation. *J. Struct. Chem.* **1993**, *34*, 359−362.
(68) Tachikawa, H.; Abe, S. Ozone−Water 1:1 Complexes O_3−H_2O: An Ab Initio study. *Inorg. Chem.* **2003**, *42*, 2188−2190.
(69) Tachikawa, H.; Abe, S. Structures and Excitation Energies of Ozone−Water Clusters $O_3(H_2O)_n$ (n = 1−4). *Inorg. Chim. Acta* **2005**, *358*, 288−294.
(70) Tachikawa, H.; Abe, S. Spectral Shifts of Ozone Molecule by the Complex Formation with a Water Molecule. *Chem. Phys. Lett.* **2006**, *432*, 409−413.
(71) Ryabinkin, I. G.; Novakovskaya, Y. V.; Stepanov, N. F. Possible Transformations of the Ozone Molecule in the Presence of Water Associates. *Russ. J. Phys. Chem.* **2006**, *80*, 106−114.
(72) Loboda, O. A.; Goncharuk, V. V. Theoretical Research into Interaction of Water Clusters with Ozone. *J. Water Chem. Technol.* **2009**, *31*, 213−219.
(73) Kumar, P.; Sathyamurthy, N. An Ab Initio Quantum Chemical Investigation of the Structure and Stability of Ozone−Water Complexes. *Chem. Phys.* **2013**, *415*, 214−221.
(74) Schmidt, M. W.; Baldridge, K. K.; Boatz, J. A.; Elbert, S. T.; Gordon, M. S.; Jensen, J. H.; Koseki, S.; Matsunaga, N.; Nguyen, K. A.; Su, S. J.; Windus, T. L.; Dupuis, M.; Montgomery, J. A. General Atomic and Molecular Electronic-Structure System. *J. Comput. Chem.* **1993**, *14*, 1347−1363.
(75) Gordon, M. S.; Schmidt, M. W. In *Theory and Applications of Computational Chemistry, the First Forty Years*; Dykstra, C. E., Frenking, K. S. K., Scuseria, G. E., Eds.; Elsevier: Amsterdam, 2005; pp 1167−1189.
(76) Day, P. N.; Jensen, J. H.; Gordon, M. S.; Webb, S. P.; Stevens, W. J.; Krauss, M.; Garmer, D.; Basch, H.; Cohen, D. An Effective Fragment Method for Modeling Solvent Effects in Quantum Mechanical Calculations. *J. Chem. Phys.* **1996**, *105*, 1968−1986.
(77) Adamovic, I.; Freitag, M. A.; Gordon, M. S. Density Functional Theory Based Effective Fragment Potential Method. *J. Chem. Phys.* **2003**, *118*, 6725−6732.
(78) Gordon, M. S.; Freitag, M. A.; Bandyopadhyay, P.; Jensen, J. H.; Kairys, V.; Stevens, W. J. The Effective Fragment Potential Method: A QM-Based MM Approach to Modeling Environmental Effects in Chemistry. *J. Phys. Chem. A* **2001**, *105*, 293−307.
(79) Stephens, P. J.; Devlin, F. J.; Chabalowski, C. F.; Frisch, M. J. Ab-Initio Calculation of Vibrational Absorption ans Circular-Dichroism Spectra Using Density-Functional Force-Fields. *J. Phys. Chem.* **1994**, *98*, 11623−11627.

(80) Dunning, T. H.; J.; Hay, P. J. In *Methods of Electronic Structure Theory*; Schaefer, H. F., III, Ed.; Plenum Press: New York, 1977; Vol. 2.
(81) Krishnan, R.; Binkley, J. S.; Seeger, R.; Pople, J. A. Self-Consistent Molecular-Orbital Methods 0.20. Basis Set For Correlated Wave-Functions. *J. Chem. Phys.* **1980**, *72*, 650−654.
(82) Frisch, M. J.; Pople, J. A.; Binkley, J. S. Self-Consistent Molecular Orbital methods 25: Supplementary Functions for Gaussian Basis Sets. *J. Chem. Phys.* **1984**, *80*, 3265−3269.
(83) Hehre, W. J.; Radom, L.; Schleyer, P. v. R.; Pople, J. A. In *Ab Initio Molecular Orbital Theory*; John Wiley: New York, 1986; pp 86−87.
(84) Dunning, T. H. J. Gaussian-Basis Sets for Use in Correlated Molecular Calculations 1. The Atmo Boron Trough Neon and Hydrogend. *J. Chem. Phys.* **1989**, *90*, 1007.
(85) Kendall, R. A.; Dunning, T. H.; Harrison, R. J. Electron-Affinities of the 1 St-Row Atoms Revisited - Systematic Basis-Sets and Wave-Functions. *J. Chem. Phys.* **1992**, *96*, 6796−6806.
(86) Cizek, J. On the Use of the Cluster Expansion and the Technique of Diagrams in Calculations of Correlation Effects in Atoms and Molecules. *Adv. Chem. Phys.* **1969**, *14*, 35.
(87) Barlett, R. J. Many-Body Perturbation Theory and Coupled Cluster Theory for Electron Correlation in Molecules. *Annu. Rev. Phys. Chem.* **1981**, *32*, 359−401.
(88) Pople, J. A.; Krishnan, R.; Schlegel, H. B.; Binkley, J. S. Electron Correlation Theories and Their Application to the Study of Simple Reaction Potential Surfaces. *Int. J. Quantum Chem.* **1978**, *14*, 545−560.
(89) Pople, J. A.; Head-Gordon, M.; Raghavachari, K. Quadratic Configuration Interaction: Reply to Commant by Paldus, Cizek, and Jeziorski. *J. Chem. Phys.* **1989**, *90*, 4635−4636.
(90) Bak, K. L.; Gauss, J.; Jorgensen, P.; Olsen, J.; Helgaker, T.; Stanton, J. F. The Accurate Determination of Molecular Equilibrium Structures. *J. Chem. Phys.* **2001**, *114*, 6548−655.
(91) Rienstra-Kiracofe, J. C.; Allen, W. D.; Schaefer, H. F., III The C_2H_5 + O_2 Reaction Mechanism: High Level Ab-Initio Characterizations. *J. Phys. Chem. A* **2000**, *104*, 9823−9840.
(92) Frisch, M. J.; Trucks, G. W.; Schlegel, H. B.; Scuseria, G. E.; Robb, M. A.; Cheeseman, J. R.; Montgomery, J. A.; J.; Vreven, T.; Kudin, K. N.; Burant, et al. *Gaussian 03*, Revision C.01; Gaussian, Inc.: Wallingford, CT, 2004.
(93) Reed, A. E.; Curtiss, L. A.; Weinhold, F. Intermolecular Interactioins from a Natural Bond orbital, Donor-Acceptor Viewpoint. *Chem. Rev.* **1988**, *88*, 899−926.
(94) Bader, R. F. W. *Atoms in Molecules. A Quantum theory*; Clarendon Press: Oxford, 1995; Vol. 22.
(95) Bader, R. F. W. *AIMPAC*, http://www.chemistry.mcmaster.ca/aimpac: downloaded May 2002.
(96) Mills, N. *J. Am. Chem. Soc.* **2006**, *128*, 13649−13650 ChemDraw Ultra 10.0; CambridgeSoft: Cambridge, MA; www.cambridgesoft.com.
(97) Hunter, J. D. Matplotlib: A 2D Graphivs Environbment. *Comput. Sci. Eng* **2007**, *9*, 90−95.
(98) Gordon, M. S.; Slipchenko, L. V.; Li, H.; Jensen, J. H. The Effective Fragment Potential: A General Method for Predicting Intermolecular Forces. *Ann. Rep. Comput. Chem.* **2007**, *3*, 177−193.
(99) Ghosh, D.; Kosenkov, D.; Vanovschi, V.; Williams, C. F.; Herbert, J. M.; Gordon, M. S.; Schmidt, M. W.; Slipchenko, L. V.; Krylov, A. I. Noncovalent Interactions in Extended Systems Described by the Effective Fragment Potential Method: Theory and Application to Nucleobase Oligomers. *J. Phys. Chem. A* **2010**, *114*, 12739−12754.
(100) Freitag, M. A.; Gordon, M. S.; Jensen, J. H.; Stevens, W. J. Evaluation of Charge Penetration Between Distributed Multipolar Expansions. *J. Chem. Phys.* **2000**, *112*, 7300−7306.
(101) Slipchenko, L. V.; Gordon, M. S. Electrostatic Energy in the Effective Fragment Potential Method: Theory and Application to Benzene Dimer. *J. Comput. Chem.* **2007**, *28*, 276−291.
(102) Slipchenko, L. V.; Gordon, M. S. Damping Functions in the Effective Fragment Potential Method. *Mol. Phys.* **2009**, *107*, 999−1016.
(103) Flick, J. C.; Kosenkov, D.; Hohenstein, E. G.; Sherrill, C. D.; Slipchenko, L. V. Accurate Prediction of Noncovalent Interaction Energies with the Effective Fragment Potential Method: Comparison of Energy Components to Symmetry-Adapted Perturbation Theory for the S22 Test Set. *J. Chem. Theor. Comput.* **2012**, *8*, 2835−2843.
(104) Hands, M. D.; Slipchenko, L. V. Intermolecular Interactions in Complex Liquids: Effective Fragment Potential Investigation of Water−tert-Butanol Mixtures. *J. Phys. Chem. B* **2012**, *116* (9), 2775−2786.
(105) Hehre, W. J.; Ditchfield, R.; Pople, J. A. Self-Consistent Molecular-Orbital Methods 0.12. Further Extensions of Gaussian-Type Basis Sets for Use in Molecular-Orbital Studies of Organic-Molecules. *J. Chem. Phys.* **1972**, *56*, 2257.
(106) Hariharan, P. C.; Pople, J. A. Influence of Polarization Functions on Molecular-Orbital Hydrogenation Energies. *Theor. Chim. Acta* **1973**, *28*, 213−222.
(107) Clark, T.; Chandrasekhar, J.; Spitznagel, G. W.; Schleyer, P. V. Efficient Diffuse Function-Augmented Basis-Sets for Anion Calculations 0.3. The 3-21+G Basis Set for 1st-Row Elements, Li-F. *J. Comput. Chem.* **1983**, *4*, 294−301.
(108) Krishnan, R.; Binkley, J. S.; Seeger, R.; Pople, J. A. Self-Consistent Molecular-Orbital Methods 0.20. Basis Set for Correlated Wave-Functions. *J. Chem. Phys.* **1980**, *72*, 650−654.
(109) Frisch, M. J.; Pople, J. A.; Binkley, J. S. Self-Consistent Molecular-Orbital Methods 0.25. Supplementary Functions for Gaussian-Basis Sets. *J. Chem. Phys.* **1984**, *80* (7), 3265−3269.
(110) Odutola, J. A.; Dyke, T. R. Partially Deuterated Water Dimers - Microwave-Spectra and Structure. *J. Chem. Phys.* **1980**, *72*, 5062−5070.
(111) Lane, J. R.; Kjaergaard, H. G. Explicitly Correlated Intermolecular Sistances and Interaction Energies of Hydrogen Bonded Complexes. *J. Chem. Phys.* **2009**, *131*, 034307.
(112) Ruscic, B., Active Thermochemical Tables: Water and Water Dimer. *J. Phys. Chem. A* **2013**, published in the web at July 8, 2013. DOI: 10.1021/jp403197t.
(113) Steiner, T. The Hydrogen Bond in the Solid State. *Angew. Chem., Int. Ed.* **2002**, *41*, 48−76.
(114) Koch, U.; Popelier, P. L. A. Characterization of C−H−O Hydrogen Bonds on the Basis of the Charge-Density. *J. Phys. Chem.* **1995**, *99*, 9747−9754.
(115) Bone, R. G. A.; Bader, R. F. W. Identifying and Analyzing Intermolecular Bonding Interactions in van der Waals Molecules. *J. Phys. Chem.* **1996**, *100*, 10892−10911.
(116) Tsyganenko, A. A.; Storozheva, E. N.; Manoilova, O. V. Manifestations of the Acidity of Adsorbed Molecules in H-Bonded Complexes with Silanol Groups: Lewis Acidity of Ozone. *Catal. Today* **2001**, *70* (1−3), 59−71.
(117) Anglada, J. The Gas Phase HO-Initiated Oxidation of Furan: A Theoretical Investigation on the Reaction Mechanism. *The Open Chemical Physics Journal* **2008**, *1*, 80−93.
(118) Merrick, J. P.; Moran, D.; Radom, L. An Evaluation of Harmonic Vibrational Frequency Scale Factors. *J. Phys. Chem. A* **2007**, *111*, 11683−11700.
(119) Pfeilsticker, K.; Lotter, A.; Peters, C.; Bosch, H. Atmospheric Detection of Water Dimers Via Near-InfraredAbsorption. *Science* **2003**, *300*, 2078−2080.
(120) Ptashnik, I. V.; Smith, K. M.; Shine, K. P.; Newnham, D. A. Laboratory Measurements of Water Vapour Continuum Absorption in Spectral Region 5000−5600 cm^{-1}: Evidence for Water Dimers. *Q. J. R. Meteorol. Soc.* **2004**, *130*, 2391−2408.
(121) Scribano, Y.; Goldman, N.; Saykally, R. J.; Leforestier, C. Water Dimers in the Atmosphere III: Equilibrium Constant from a Flexible Potential. *J. Phys. Chem. A* **2006**, *110*, 5411−5419.
(122) Vaida, V.; Headrick, J. E. Physicochemical Properties of Hydrated Complexes in the Earth's Atmosphere. *J. Phys. Chem. A* **2000**, *104*, 5401−5412.
(123) Goldman, N.; Fellers, R. S.; Leforestier, C.; Saykally, R. J. Water Dimers in the Atmosphere: Equilibrium Constant for Water Dimerization from the VRT (ASP-W) Potential Surface. *J. Phys. Chem. A* **2001**, *105*, 515−519.